

## Salt Waters of the Northern Apennine Foredeep Basin (Italy): Origin and Evolution

Tiziano Boschetti · Lorenzo Toscani · Orfan Shouakar-Stash ·  
Paola Iacumin · Giampiero Venturelli · Claudio Mucchino ·  
Shaun K. Frape

Received: 17 December 2009/Accepted: 19 July 2010/Published online: 21 August 2010  
© Springer Science+Business Media B.V. 2010

**Abstract** The salt waters from the Emilia-Romagna sector of the Northern Apennine Foredeep have been investigated using major and trace element and stable isotope ( $\delta^2\text{H}$ ,  $\delta^{18}\text{O}$ ,  $\delta^{37}\text{Cl}$ ,  $\delta^{81}\text{Br}$  and  $^{87}\text{Sr}/^{86}\text{Sr}$  ratio). Ca, Mg, Na, K, Sr, Li, B, I, Br and  $\text{SO}_4$  vs. Cl diagrams suggest the subaerial evaporation of seawater beyond gypsum and before halite precipitation as primary process to explain the brine's salinity, whereas saline to brackish waters were formed by mixing of evaporated seawater and water of meteoric origin. A diagenetic end-member may be a third component for mud volcanoes and some brackish waters. Salinization by dissolution of (Triassic) evaporites has been detected only in samples from the Tuscan side of the Apennines and/or interacting with the Tuscan Nappe. In comparison with the seawater evaporation path, Ca–Sr enrichment and Na–K–Mg depletion of the foredeep waters reveal the presence of secondary processes such as dolomitization–chloritization, zeolitization–albitization and illitization. Sulfate concentration, formerly buffered by gypsum-anhydrite deposition, is heavily lowered by bacterial and locally by thermochemical reduction during burial diagenesis. From an isotopic point of view, data of the water molecule confirm mixing between seawater and meteoric end-members. Local  $^{18}\text{O}$ -shift up to +11‰ at Salsomaggiore is related to water–rock interaction at high temperature ( $\approx 150^\circ\text{C}$ ) as confirmed by chemical (Mg, Li, Ca distribution) and isotopic ( $\text{SO}_4-\text{H}_2\text{O}$ ) geothermometers.  $^{37}\text{Cl}/^{35}\text{Cl}$  and  $^{81}\text{Br}/^{79}\text{Br}$  ratios corroborate the

---

**Electronic supplementary material** The online version of this article (doi:[10.1007/s10498-010-9107-y](https://doi.org/10.1007/s10498-010-9107-y)) contains supplementary material, which is available to authorized users.

T. Boschetti (✉) · L. Toscani · P. Iacumin · G. Venturelli  
Department of Earth Sciences, University of Parma, 157a via GP Usberti, 43100 Parma, Italy  
e-mail: work@tizianoboschetti.com

O. Shouakar-Stash · S. K. Frape  
Department of Earth Sciences, University of Waterloo, 200 University Avenue W., Waterloo,  
ON N2L 3G1, Canada

C. Mucchino  
Department of Analytical Chemistry, University of Parma, 17a via GP Usberti, 43100 Parma, Italy

marine origin of the brines and evidence the diffusion of halogens from the deepest and most saline aquifers toward the surface. The  $^{87}\text{Sr}/^{86}\text{Sr}$  ratio suggests a Miocene origin of Sr and rule out the hypothesis of a Triassic provenance of the dissolved components for the analyzed waters issuing from the Emilia-Romagna sector of the foredeep. Waters issuing from the Tuscan side of the Apennines and from the Marche sector of the foredeep show higher  $^{87}\text{Sr}/^{86}\text{Sr}$  ratios because of the interaction with siliciclastic rocks.

**Keywords** Salt waters · Chemical and isotope composition · Seawater evaporation · Northern Apennine Foredeep

## 1 Introduction

The presence of salt waters in the Northern Apennine and its foredeep (Po Basin) is known since Roman and Middle Age times, when they were used for thermal and therapeutic purposes or for salt collection (Artusi et al. 1977; Rosetti and Valenti 2002). More recently, they have been extensively studied for their association with methane and petroleum hydrocarbons (Agip Mineraria 1959), their possible association with seismic activity (mud volcanoes) and the potential of host formation as carbon sinks. Despite these main topics, a clear explanation of the origin of these waters is still lacking. During hydrocarbon research, brines were widely intercepted in the Po Basin (Fig. 1; Agip Mineraria 1959), and those with highest salinity were found in a relatively restricted area of the Emilia sector of N-Apennine Foredeep between the provinces of Parma (Monticelli: up to 130 g/L, Fontevivo: up to 167 g/L, Salsomaggiore: up to 190 g/L; Iacumin et al. 2007; Toscani et al. 2007) and Piacenza (Cortemaggiore: up to 233 g/L; Pieri 1992). Other brines occur also in the Marche sector of N-Apennine Foredeep (Tolentino: up to 197 g/L; Nanni and Vivalda 1999). Unfortunately, most of the wells are not available for sampling at present (i.e. Cortemaggiore, Fontevivo), but salt waters from spas are available (i.e. Salsomaggiore, Monticelli, Tolentino).

In this paper, we investigate 26 sites of Br–I-rich sodium-chloride brackish to brine waters issuing from springs and wells of the Northern Apennine and its foredeep (underlined codes in Fig. 1) in order to characterize them both chemically and isotopically, investigate their origin and evolution (the mechanism of water salinization (salt enrichment in water) and the role of water–rock interaction) and define, if possible, the geological evolution of the aquifers. Waters sampled in the Emilia-Romagna Region are from Bacedasco Terme, Salsominore and Bobbio (BAC, SALMIN, BOB, Piacenza Province), Sant'Andrea Bagni, Salsomaggiore Terme, Lesignano and Monticelli Terme (F11 and F12, SALMAG, LES, MONT, respectively, Parma Province), Quara (F15, Reggio-Emilia Province), Salvarola Terme (SALV, Modena Province), Castello di Serravalle and Castel San Pietro Terme (SER, CSP, Bologna Province), Riolo Terme, Casola Valsenio, Brisighella and Punta Marina Terme (RIT, CSV, BR, PMT, Ravenna Province), Castrocaro Terme, Fratta Terme and Panighina (CC, FRA, PAN, Forlì-Cesena Province), Terme di Riccione and Terme di Rimini (MIR, ISA and CLA, respectively, Rimini Province) and Terme di Montegrimano (MGR, Pesaro-Urbino Province). In addition, the water of the “Terme di S. Lucia” (SL13 and SL14, Tolentino, Macerata Province) outpouring from the Marche side of the Northern Apennine Foredeep and three saline waters from “Terme della Versilia”, Bergondola and Ponte Magra from the Tuscan side of the Northern Apennine (VER, BERG and PM, Massa-Carrara Province) have been sampled for comparison.

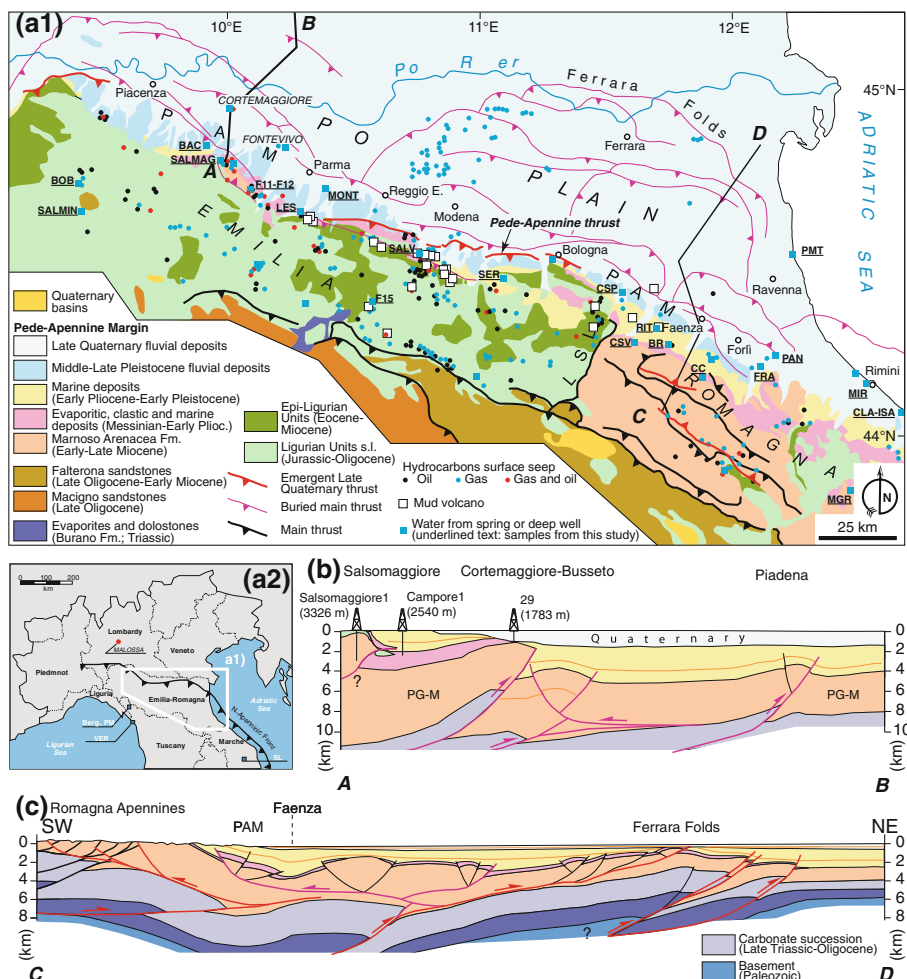


**Fig. 1** **a1** Geological map of the Northern Apennine and its foredeep (modified after Bonini 2007). Underlined codes refer to salt water samples of this study; *PAM* Pede-Apennine Margin; *LSL* Livorno-Sillaro lineament. **a2** Northern Italy and samples which do not belong to the Po River Basin. **b** and **c** cross-sections *A–B* and *C–D*, respectively. PG-M, undifferentiated Paleogene-Miocene sediments (**b**)

## 2 Geological and Hydrological Setting

The Po Basin (Northern Italy, Fig. 1) covers an area of approximately 46,000 km<sup>2</sup> and is bound to the N by the Alps, to the SW by the Apennines and to the E by the Adriatic Sea. Springs and wells investigated in this paper occur over a distance of about 300 km, from the Province of Piacenza to the Province of Rimini, along the northeastern margin of the Apennine and in the Po Plain (Fig. 1) corresponding to the Northern Apennine Foredeep (e.g. Roveri et al. 2001). Hereafter, the synthetic description of the main geological domains, lithology and tectonic evolution of the Apennine chain is reported since they are fundamental in supporting the geochemical investigation into the salt waters as for other fluids of the Apennine (Duchi et al. 2005).

The Apennine chain is a thrust and fold belt composed of several units, structurally homogeneous, that were emplaced toward N-NE from Early Cretaceous to present during the closure of the Piedmont-Ligurian ocean and the collision of the European and Adria plates. In the northwestern Apennines, the allochthonous Ligurian Internal units (Mesozoic oceanic and forearc sedimentary deposits) and the overlying Epiligurian units (Middle Eocene-Early Messinian turbidites and shallow water primary evaporites) represent the upper structural level that translated on the foredeep, reached the foreland and overthrust the foredeep more recent turbidites (e.g. Argnani and Ricci Lucchi 2001). In the Salsomaggiore anticline (Fig. 1b), the Serravallian-Langhian deposits were overrode in the Messinian and newly exposed in the Pliocene–Pleistocene (Artoni et al. 2004). The lower structural level of the Apennines corresponds to the Tuscan(nappe)-Umbrian( foredeep) units consisting of crystalline rocks of the metamorphic Paleozoic basement and Mesozoic carbonates (Triassic evaporite and dolostone, Fig. 1a). The rocks of the Tuscan domain are exposed in some tectonic windows of the Ligurian units; for example, near Bobbio, Piacenza Province and at the Mt. Zuccone, Parma Province. Oligo-Miocene turbidite formations are related to the infill stages of the eastward-migrating foredeep in front of the advancing Apenninic orogenic stack of the nappes. In the western sector of the Northern Apennine, the Macigno Formation characterizes the top of the Tuscan Nappe. The Romagna Apennines (east of the Sillaro Valley) are mainly composed by the Marnoso-Arenacea turbiditic formation (Langhian-Tortonian: Ricci Lucchi 1981) overlying the basement of Miocene carbonates and overlaid by Macigno, Modino and Cervarola turbidites in the inner parts (Apennine ridge). Messinian to Pleistocene deposits (N-NE dipping) cover the Marnoso-Arenacea formation along the NE Apennine foothills (Roveri et al. 2003). The outermost front of the Northern Apennine (several anticlines roughly oriented WNW-ESE) is buried by Pliocene–Pleistocene marine sediments under the surface of the Po Plain (Fig. 1c).

The surface hydrology of Emilia-Romagna region is formed of rivers draining the Apennines with their alluvial fans. The alluvial fans that formed the Po valley are interbedded, and their northern ends are connected with the Quaternary sediments of the Po river. The groundwaters exploited for drinking-water supply are classified into three main hydrostratigraphic units (Emilia-Romagna 1998); the two deepest, known as aquifer B (from 0.35–0.45 to 0.65 Ma) and aquifer C (from 0.65 to 3.9 Ma), occupy parallel bands in the middle plain and near the Apennines, respectively. The bottom of the deepest unit is known as “basal aquitard” (>3.9 Ma) and defines a low permeable unit, unexploited for drinking due to great depth and possible mixing with salt waters, which is the subject of this paper.

### 3 Analytical Methods

#### 3.1 Field Methods

All water samples were filtered through 0.45- $\mu\text{m}$  cellulose acetate filters, and the portion devoted to cation analysis was acidified with 65% HNO<sub>3</sub> Suprapur Merck. Reduced dissolved N(-III) was determined by spectrophotometry using a portable photometer (MERCK SQ300 with Spectroquant kits), whereas S(-II) species and by iodometric method. Temperature, pH and Eh were determined using an Orion 250A instrument equipped with a Ross glass electrode for pH and a Orion 91-79 Triode<sup>TM</sup> (Thermo Scientific) electrode for Eh determination (platinum redox sensor, silver/silver chloride internal reference system and built-in thermistor for automatic temperature compensation).

The electrode for Eh was calibrated with an Orion ORP Standard (at 25°C, Eh = +420 mV relative to standard hydrogen electrode). Specific conductance (at 20°C) was measured using a YELLOW SPRING 85 conductivity meter. Total alkalinity was determined in the field by acidimetric titration and in the laboratory by Gran titration (Gran 1952) not later than 12 h after sampling.

### 3.2 Density, Major and Trace Element Analyses

Density was measured by pycnometers at 20 ± 1°C, silica by spectrophotometry (MERCK SQ300 with Spectroquant kit) and Na, K, Ca, Mg, S, Li, B, Mn, Fe, Sr, Ba, Zn, As by ICP-OES (Inductively Coupled Plasma Optical Emission Spectrometry). Cl was determined by the Mohr's method, total I and Br by flow injection ICP-MS coupled with a gradient pump DIONEX GP-40 and an automatic injection valve ERC iVALVE (for details, Boschetti 2003). Radon (<sup>222</sup>Rn) was determined by ionization chamber alpha particles detector (AlphaGUARD- Genitron Instruments; Health Physics Service of the University of Parma; Vaccari et al. 1999). Total dissolved carbon and total dissolved nitrogen were measured by elemental analysis with automatic liquid injection using FlashEA 1112 elemental analyzer equipped with an AS3000 liquid autosampler (Thermo Fisher Scientific).

### 3.3 Isotopes

The delta isotope composition of hydrogen and oxygen ( $\delta^2\text{Hc}$  and  $\delta^{18}\text{Oc}$ ), which is not affected by salt effect, was obtained making isotope determination on the distilled samples. Salt water samples were distilled in a vacuum line (1 h at 100°C, then 1 h at 370°C) and condensed in a liquid nitrogen cryogenic trap. Afterward, the condensed water samples were transferred on a FINNIGAN GLF 1086 automatic equilibration device on line with a DELTA PLUS FINNIGAN mass-spectrometer. In this analytic line, hydrogen for  $\delta^2\text{H-c}$  determination was obtained by H<sub>2</sub>-water equilibration using a Pt-rich catalyst, while  $\delta^{18}\text{O-c}$  determination was carried out on CO<sub>2</sub>-water equilibration at 18°C (Epstein and Mayeda 1953). Data are referred to V-SMOW, and standard errors are about ±1.0‰ and better than ±0.1‰ for  $\delta^2\text{H-c}$  and  $\delta^{18}\text{O-c}$ , respectively.

The method has been checked by monthly analyses of the most saline brines from Monticelli and Salsomaggiore that gave a standard deviation of ±0.20 and ±0.23 for oxygen and ±1.3 and ±1.6 for hydrogen, respectively (Iacumin et al. 2007). The salt effect parameter  $10^3\ln\Gamma$  (Horita et al. 1993) on the saline and brine samples was calculated at the temperature of sampling by EQ3/6 code with the Pitzer database (see next section). The calculated δ-activity (δa) ratio  $\delta a = \delta c + 10^3\ln\Gamma$  (Table 2) shows that the salt effect on oxygen is within analytical uncertainty probably due to lacking or low content of sulfate species in the solutions; whereas salt effect reaches 4.3–5.6‰ on the hydrogen of the brines.

Chlorine stable isotope analyses were performed on methyl chloride (CH<sub>3</sub>Cl) gas following the procedure described in Eggenkamp (1994) and Shouakar-Stash et al. (2005b). Bromine stable isotope analyses were carried out on methyl bromide (CH<sub>3</sub>Br) gas using a continuous flow—isotope ratio mass spectrometry (CF-IRMS) (IsoPrime, Micromass—currently Elementar-, UK) following Shouakar-Stash et al. (2005a). Both chlorine and bromine stable isotopes were reported relative to standard mean ocean chloride (SMOC) and bromide (SMOB), respectively. The analytical precisions for both <sup>37</sup>Cl and <sup>81</sup>Br isotopes are 0.1‰.

Strontrium stable isotopes were analyzed by TIMS (Thermal Ionization Mass Spectroscopy, Triton Thermo-Finnigan) at the University of Waterloo following an in-house analytical protocol (El Mugammar and Shouakar-Stash 2008; analytical uncertainty better than 0.00005).

Oxygen and sulfur isotope of dissolved sulfate were analyzed also for the SALMAG brines by CF-IRMS after precipitation as BaSO<sub>4</sub> (for details, see Boschetti et al. 2010).

### 3.4 Thermodynamic Calculations

Dissolved species activities and mineral saturation indexes were calculated by EQ3/6 software with the YPF thermodynamic database (based on the Pitzer formalism for activity calculation; Wolery and Jarek 2003). Carbonate alkalinity was early calculated by PHREEQCI software (Parkhurst and Appelo 1999) using LLNL database and total carbon or total alkalinity. However, as Pitzer database lack pressure correction, the B-dot equation for computing of activity coefficients coupled with the specific pressure corrected thermodynamic database data0.500 was also applied for the activity calculation of the dissolved species (EQ3/6 software, Wolery and Jarek 2003). In this latter case, the thermodynamic database was implemented with the solubility constant of the reaction C<sub>2</sub>H<sub>6</sub>(g)=C<sub>2</sub>H<sub>6</sub>(aq) from OBIGT database (<http://affinity.berkeley.edu/predcent/download/obigt>). Additional thermodynamic data of the minerals used for activity diagrams are from thermo.com.v8.r6.dat, thermo.dat ([http://www.geology.uiuc.edu/Hydrogeology/hydro\\_thermo.htm](http://www.geology.uiuc.edu/Hydrogeology/hydro_thermo.htm)) and THERMODDEM database (illite-Mg; <http://thermoddem.brgm.fr>).

## 4 Results

Chemical composition of the investigated waters is reported in Table 1; the isotope data are reported in Table 2. Waters can be divided into brine (TDS > 100 g/L; MONT, SL4 and SALMAG), saline (20 < TDS < 100 g/L; FRA, SL13, CC, BR, CSP, RIT, ISA) and brackish (TDS < 20 g/L; BAC, MIR, MGR, SER, BOB, CLA, PAN, PTM, CSV, PM, SALV, BERG, VER, SALMIN) according to the classification of Drever (1997). With the exception of samples BAC and F11 (waters of Na-C-HCO<sub>3</sub> type), all waters are of Na-Cl type (Fig. 2), hypothermal (13.6–21.1°C, Schoeller 1962) and neutral to slightly basic (pH = 6.70–8.64); the brines are also Ca-Cl having equivalent ratio Ca/(SO<sub>4</sub> + HCO<sub>3</sub>) > 1. Major cations are roughly correlated with Cl<sup>-</sup>. Total sulfur reaches the highest content in the brackish waters of PAN, CSV, VER and BERG (S = 258, 101, 455, 124 mg/L, respectively) and S(-II) in the CLA springs (total H<sub>2</sub>S = 14.3 mg/L). Reduced N(-III) is roughly correlated with TDS. The brines, some saline and brackish waters (SALMIN and SALV) have the highest contents of Br (up to 480 mg/L), Li (up to 96.4 mg/L) and B (up to 373 mg/L). The distribution of iodine is unrelated to salinity being the highest I contents detected at CSP, CSV and SALMAG (147, 138 and 111 mg/L, respectively). Sr and Ba are roughly related to Ca in all waters and reach the highest content in the saline and brine samples (SL samples; Sr = 553 mg/L at SL4; Ba = 929 mg/L at SL13). Among the elements of the first transition series, only Fe and Mn occur in significant amount in brines (up to 33 and 3.8 mg/L for Fe and Mn, respectively).

According to Hanor (1987), comparison of seawater and brines formed by evaporation of seawater is a valid technique to investigate the origin and composition variability of many waters from sedimentary basins. In the diagrams element vs. chlorine (Fig. 3), where

**Table 1** Chemical composition of the sampled waters arranged by increasing salinity: brackish ( $1 < \text{TDS} < 20 \text{ g/L}$ ), saline ( $20 < \text{TDS} < 100 \text{ g/L}$ ) and brine ( $\text{TDS} > 100 \text{ g/L}$ )

Code	Name-locality (Province)	Cond. (mS/cm)	TDS (g/L)	Density (g/cm <sup>3</sup> )	T (°C)	pH (T water)	Eh (mV)	Ca (mg/L)	Mg (mg/L)	Na (mg/L)	K (mg/L)	tAlk (mg/L as HCO <sub>3</sub> <sup>-</sup> )	Cl (mg/L)	H <sub>2</sub> S <sub>c</sub> (mg/L)*	N (-II) (mg/L)
<i>Brackish waters</i>															
BAC1	Bacedasco Ex spa (PC)	2.04	1.1	0.996	13.2	7.34	44	60	52	300	15	560	330	11.0	<0.05
F11	St. Andrea Bagni (PR)	1.90	1.2	—	16.0	9.00	−89	2.2	1.9	464	4.5	540	321	—	—
MIR1	Rimini spa (RN)	3.74	1.7	0.997	14.8	7.35	175	131	87	397	11	674	750	—	2.0
MGR	Montegriniano spa (PU)	6.23	3.6	0.999	13.3	7.01	325	107	48	1,440	7	867	1,460	8.9	1.7
F15_01	Quara-Toano (RE)	8.90	6.9	—	14.0	7.40	—	23	9.8	2,606	56	771	3,802	—	—
F15_02	=	10.2	7.1	—	10.7	7.34	—	32	8.3	2,559	57	766	4,059	—	—
SER1	Castello di Serravalle (BO)	13.3	7.8	1.000	14.5	8.10	233	24	88	2,800	43	1082	4,313	—	2.6
LES	Lesignano de' Bagni (PR)	—	9.0	—	—	—	—	268	135	3,031	29	761	5,123	—	—
BOB1	Bobbio (PC)	17.0	9.8	1.003	20.5	6.97	−154	328	41	3,220	103	347	5,909	7.0	<0.05
CLA1	Riccione spa (RN)	18.1	10.9	1.003	15.6	7.00	60	425	384	3,120	45	565	6,622	14.3	<0.05
PAN1	Panighina-Bertinoro (FC)	20.2	11.8	1.004	19.4	7.71	55	791	345	3,190	64	173	7,234	1.0	<0.05
PMT1	Punta Marina spa (RA)	22.8	13.6	1.005	16.5	7.41	53	207	555	4,210	45	365	8,422	—	7.4
CSV1	Casola Valsenio (RA)	22.7	13.9	1.005	15.4	7.77	−53	95	271	4,920	119	910	7,981	9.1	17
PM2	Mulazzo (MS)	23.1	14.2	1.009	16.8	7.84	−30	210	113	5,210	28	86	8,589	1.2	8.3
CSV2	Casola Valsenio (RA)	22.1	15.2	1.004	14.0	7.61	—	103	280	5,510	132	947	8,660	—	24
SALV1	Salvarola spa (MO)	25.0	15.5	1.007	15.3	8.37	227	4.7	13	5,950	18	2079	8,490	12.9	1.9
BERG1	Bergondola (MS)	26.2	16.0	1.007	14.2	7.24	234	662	89	5,220	49	52	9,848	—	5.0
SALV2	Salvarola spa (MO)	23.2	16.3	1.003	15.7	8.34	134	7.8	14	6,540	16	2089	8,626	13.0	0.7
VER01	Versilia spa—Cinqueale (MS)	28.6	16.4	1.009	16.8	7.32	250	328	544	5,320	160	300	9,781	—	3.2
BERG2	Mulazzo (MS)	24.2	16.6	1.005	15.3	7.50	4	740	90	5,730	52	49	9,902	0.6	5.6

**Table 1** continued

Code	Name-locality (Province)	Cond. (mS/cm)	TDS (g/L)	Density (g/cm <sup>3</sup> )	T (°C)	pH (T water)	Eh (mV)	Ca (mg/L)	Mg (mg/L)	Na (mg/L)	K (mg/L)	tALK (mg/L as HCO <sub>3</sub> <sup>-</sup> )	Cl (mg/L)	H <sub>2</sub> S <sub>I</sub> (mg/L)	N (-III) (mg/L)*
F12	St. Andrea Bagni (PR)	22.0	17.6	—	10.7	7.53	-104	340	183	6,590	33	199	10,307	—	—
SALMINI	Salsomignore-Ferrriere (PC)	29.2	17.9	1,008	21.1	6.70	24	701	93	5,860	225	267	10,867	—	17
<i>Saline waters</i>															
ISA1	Riccione spa (RN)	35.5	22.2	1,011	16.0	7.00	55	553	695	6,720	114	613	13,822	3.6	<0.05
RT1	Riolo Terme spa (RA)	47.2	30.6	1,017	19.4	7.64	40	256	718	10,200	232	423	18,882	—	42
CSP1	Castel S.Pietro spa (BO)	50.0	32.6	1,019	20.3	7.70	92	311	606	11,000	185	430	20,206	—	54
CSP2	=	50.8	32.7	1,022	20.6	7.45	103	330	659	11,300	210	425	19,969	—	52
CC1	Castrocaro Terme spa (RA)	62.5	43.1	1,025	13.6	7.19	-70	870	767	14,700	129	239	26,421	8.7	34
BRI	Brisighella spa (RA)	67.2	47.5	1,030	16.3	8.64	149	1,640	1,070	15,100	74	215	29,444	—	64
SL13	S. Lucia spa—Tolentino (MC)	90.0	72.6	1,044	13.1	6.68	-33	3,801	1,237	21,147	101	87	45,666	0.9	107
FRA2	Fratta Terme spa (FC)	90.2	73.6	1,046	15.2	7.25	135	2,020	1,230	25,500	230	153	44,488	11.9	82
FRA2As	=	92.8	75.0	1,050	12.8	6.70	93	1,780	1,080	23,500	219	123	47,394	10.5	88
FRA1	=	103.9	81.1	1,054	16.2	6.88	180	2,520	1,500	25,600	219	157	51,026	6.0	91
<i>Brine waters</i>															
MONT1	Monticelli spa (PR)	140.5	116	1,080	15.8	6.83	130	5,670	2,470	34,500	234	57	73,015	—	82
SL4	S. Lucia spa—Tolentino (MC)	133.2	118	1,093	13.7	6.23	270	5,752	2,301	35,732	164	87	74,374	2.4	50
27SALMAGI	Salsomaggiore spa (PR)	152.9	131	1,090	16.9	7.16	85	3,510	1,100	41,900	208	194	83,403	—	—
210SALMAGI	=	174.5	152	1,103	16.9	6.98	112	4,270	1,210	49,700	274	187	96,108	—	—

**Table 1** continued

Code	Name-locality (Province)	Total C (mg/L)	SiO <sub>2</sub> (mg/L)	Rn (Bq/L) ± st.dev.)	I (mg/L)	Br (mg/L)	Sr (mg/L)	S (mg/L)	Li (mg/L)	B (mg/L)	Mn (μg/L)	Ba (μg/L)	Fe (μg/L)	Charge balance (%)	
<i>Brackish waters</i>															
BAC1	Bacedasco Ex spa (PC)	100	<15	18.6	14.32 ± 1.00	0.87	1.98	2.10	47	0.2	62	246	86	<1	-1.4
F11	St. Andrea Bagni (PR)	—	—	10.7	—	0.38	0.88	0.29	54	0.1	2,588	8.3	97	3	-1.7
MIR1	Rimini spa (RN)	131	<15	11.9	6.05 ± 0.60	1.79	5.22	2.32	11	0.2	389	11	507	2,485	-2.2
MGR	Montegriniano spa (PU)	174	<15	7.4	0.28 ± 0.06	1.21	6.6	4.71	211	0.3	—	136	60	110	2.7
F15_01	Quara-Tano (RE)	—	—	16.7	—	—	6.49	0.94	1.6	10,531	11	9,431	14	—1.1	
F15_02	=	—	—	16.3	—	0.22	1.0	6.15	2.6	1.6	8,944	8.5	8,841	8.7	-4.8
SER1	Castello di Serravalle (BO)	211	<15	8.0	26.79 ± 1.15	0.64	19	2.42	3.1	0.3	2,916	19	2,354	97	-2.9
LES	Lesignano de' Bagni (PR)	—	—	27.3	—	—	12.4	3.0	1.2	12,821	45	9,099	301	0.2	
BOB1	Bobbio (PC)	59	<15	12.4	4.24 ± 0.50	1.07	3.66	39.9	9.6	2.3	10,088	52	6,686	10	-2.7
CLAI	Riccione spa (RN)	100	<15	11.6	11.05 ± 0.80	1.88	27	22.0	8.0	0.3	<1	850	24,185	11	-1.6
PANI	Panighina-Bertinoro (FC)	29	<15	22.2	0.84 ± 0.20	2.13	26	15.1	258	0.4	709	153	58	<1	-3.3
PMT1	Punta Marina spa (RA)	82	<15	6.4	7.36 ± 0.80	2.65	27	8.57	1.3	0.2	433	63	1,667	5,280	-0.5
CSV1	Casola Valsenio (RA)	170	15	8.2	2.17 ± 0.35	138	33	3.35	101	0.3	2,748	35	914	66	-0.2
PM2	Mulazzo (MS)	10	<15	6.4	—	0.20	2.91	55.1	32	3.6	—	104	290	80	0.7
CSV2	Casola Valsenio (RA)	—	—	7.4	—	18	42	3.65	80	0.2	—	45	1,210	—	1.5
SALV1	Salvarola spa (MO)	379	<15	11.4	35.46 ± 1.25	20.5	101	4.04	2.7	0.8	105,429	11	1,180	24	-2.4
BERG1	Bergondola (MS)	11	<15	9.3	11.92 ± 0.95	0.73	2.92	82.6	124	3.2	2,095	152	64	10.5	-2.7
SALV2	Salvarola spa (MO)	396	<15	11.0	—	—	4.33	5.6	0.7	100,000	—	—	—	—	1.6
VER01	Versilia spa—Cinquale (MS)	56	<15	7.0	7.37 ± 0.80	0.28	28	3.89	455	0.2	721	295	18	27	-2.0

**Table 1** continued

Code	Name-locality (Province)	Total C (mg/L)	Total N (mg/L)	SiO <sub>2</sub> (mg/L)	Rn (Bq/L) ± st.dev.)	I (mg/L)	Br (mg/L)	Sr (mg/L)	S (mg/L)	Li (mg/L)	B (µg/L)	Mn (µg/L)	Ba (µg/L)	Fe (µg/L)	Charge balance (%)
BERG2	Mulazzo (MS)	4	<15	8.5	—	0.11	3.14	85.6	113	3.2	2,150	223	100	—	1.8
F12	St. Andrea Bagni (PR)	—	—	13.2	—	24	36	25.0	14	0.5	33,252	60	1,904	11	4.1
SALMIN1	Salsominore- Ferriere (PC)	49	<15	12.9	52.52 ± 2.50	2.40	10	133	1.1	11.3	22,989	228	24,547	502	-0.3
<i>Saline waters</i>															
ISA1	Riccione spa (RN)	109	20	11.0	21.51 ± 1.10	8.24	80	36.3	7.0	0.4	177	738	34,128	10.0	-2.4
RTI1	Riolo Terme spa (RA)	98	36	6.2	4.20 ± 0.50	60	108	10.5	0.8	0.4	5,308	38	15,856	9,181	-1.4
CSP1	Castel S.Pietro spa (BO)	108	41	9.2	2.57 ± 0.40	147	158	16.4	0.9	0.5	7,509	77	23,904	2,554	-2.2
CSP2	=	101	51	8.1	—	59	140	15.8	1.1	0.4	—	115	24,200	2,690	0.1
CC1	Castrocaro Terme spa (RA)	52	25	8.3	3.99 ± 0.45	17	151	76.1	17	0.7	7,880	188	15,892	326	0.2
BRI1	Brisighella spa (RA)	44	35	8.7	8.76 ± 0.85	8.90	152	151	0.5	0.7	8,118	386	34,260	6,325	0.1
SL13	S. Lucia spa— Tolentino (MC)	—	—	25.1	—	16	268	184	160	1.1	11,500	902	929,000	490	-3.0
FRA2	Fratta Terme spa (FC)	29	86	8.9	5.77 ± 0.50	32	230	306	3.9	1.5	—	341	64,000	1,030	2.8
FRA2AS	=	27	82	9.1	—	29	198	279	0.9	0.9	—	252	45,500	8,100	-4.7
FRA1	=	40	77	8.0	33.78 ± 1.20	101	342	320	0.9	1.2	10,683	384	53,643	9,419	-2.1
<i>Brine waters</i>															
MONT1	Monticelli spa (PR)	20	89	7.2	—	72	480	318	0.6	2.0	17,673	3,805	93,800	32,190	-1.3
SL4	S. Lucia spa— Tolentino (MC)	—	—	9.6	—	90	362	553	5.5	4.2	8,150	1,650	74,400	5,420	-1.2

**Table 1** continued

Code	Name-locality (Province)	Total C (mg/L)	Total N (mg/L)	SiO <sub>2</sub> (mg/L)	Rn (Bq/L) ± st.dev.)	I (mg/L)	Br (mg/L)	Sr (mg/L)	S (mg/L)	Li (mg/L)	B (μg/L)	Mn (μg/L)	Ba (μg/L)	Fe (μg/L)	Charge balance (%)
27SALMAGI	Salsomaggiore spa (PR)	24	142	6.6	—	111	368	414	37	60.6	373,000	1,210	8,463	27,038	-4.9
210SALMAGI	=	15	164	5.5	0.79 ± 0.20	97	360	343	27	96.4	358,000	1,330	7,978	33,044	-3.8

With the exception of waters F11, F15 and LES (sampled during 2001–2005), all the samples were collected during October–November 2006 (number 1 as last figure in the sample code), May–July 2007 (number 2 as last figure in the sample code) and November 2007 (SL13, SL14). TDS (total dissolved solids) = [0.5 × tAlk + Ca + Mg + Na + K + Cl + SO<sub>4</sub> + (2.82 × H<sub>2</sub>S) + NH<sub>4</sub> + (1.02 × SiO<sub>2</sub>)]/1000 (g/L) (modified after APHA-AWWA-WEF 1995)

$$\text{Charge Balance} = 100 \times [\sum \text{cations} - \sum \text{anions}] / (\sum \text{cations} + \sum \text{anions}) \quad (\text{APHA-AWWA-WEF 1995})$$

“\_” not analyzed; “=” ibidem

\* Total dissolved sulfide as H<sub>2</sub>S<sub>t</sub>

**Table 2** Isotope ratios of the sampled waters

Code	$\delta^{18}\text{O}(\text{H}_2\text{O})_{\text{c}}$ ‰ vs. V-SMOW	$\delta^{18}\text{O}(\text{H}_2\text{O})_{\text{a}}$ ‰ vs. V-SMOW	$10^3 \ln \Gamma \text{ O}$	$\delta^{2}\text{H}(\text{H}_2\text{O})_{\text{c}}$ ‰ vs. V-SMOW	$\delta^{2}\text{H}(\text{H}_2\text{O})_{\text{a}}$ ‰ vs. V-SMOW	$10^3 \ln \Gamma \text{ H}$	$\delta^{37}\text{Cl}$ ‰ vs. SMOC	$\delta^{31}\text{Br}$ ‰ vs. SMOB	$87\text{Sr}/86\text{Sr}$	$\delta^{34}\text{S}(\text{SO}_4)$ ‰ vs. V-CDT	$\delta^{18}\text{O}(\text{SO}_4)$ ‰ vs. V-SMOW
<i>Brackish waters</i>											
BAC1	-9.09	-	-	-62.9	-	-	0.15	0.73	0.70904	-	-
F11	-9.53	-	-	-66.3	-	-	-	-	0.70854	-	-
MIR1	-9.95	-	-	-72.1	-	-	-1.44	-0.35	0.70887	-	-
MGR	-0.08	-	-	0.0	-	-	-	-	-	-	-
FL5_02	-8.56	-	-	-59.4	-	-	-	-	0.71092	-	-
SER1	-5.56	-	-	-40.6	-	-	-0.50	0.56	0.70876	-	-
LES	4.20	-	-	-13.1	-	-	-	-	-	-	-
BOB1	-7.87	-	-	-55.6	-	-	-0.42	0.66	0.71111	-	-
CLA1	-7.23	-	-	-47.7	-	-	-0.89	0.00	0.70899	-	-
PANI	-7.76	-	-	-53.3	-	-	-0.37	0.29	0.70907	-	-
PMT1	-5.45	-	-	-39.9	-	-	-0.16	-0.09	0.70920	-	-
CSV1	-5.92	-	-	-40.5	-	-	-0.15	0.17	0.70892	-	-
PM1	-7.80	-	-	-50.1	-	-	-	-	-	-	-
PM2	-7.82	-	-	-49.3	-	-	-	-	0.70890	-	-
CSV2	-5.70	-	-	-38.5	-	-	-	-	-	-	-
SALV1	3.66	-	-	-15.2	-	-	0.16	0.88	0.70869	-	-
BERG1	-7.50	-	-	-47.1	-	-	-0.71	0.88	0.71010	-	-
SALV2	4.00	-	-	-13.5	-	-	-	-	-	-	-
VER1	-2.57	-	-	-15.2	-	-	-0.21	0.03	0.70952	-	-
BERG2	-7.48	-	-	-47.2	-	-	-	-	0.70998	-	-
FL2	-	-	-	-	-	-	-	-	0.70911	-	-
SALMIN1	-6.93	-	-	-50.2	-	-0.31	0.12	0.71057	-	-	-

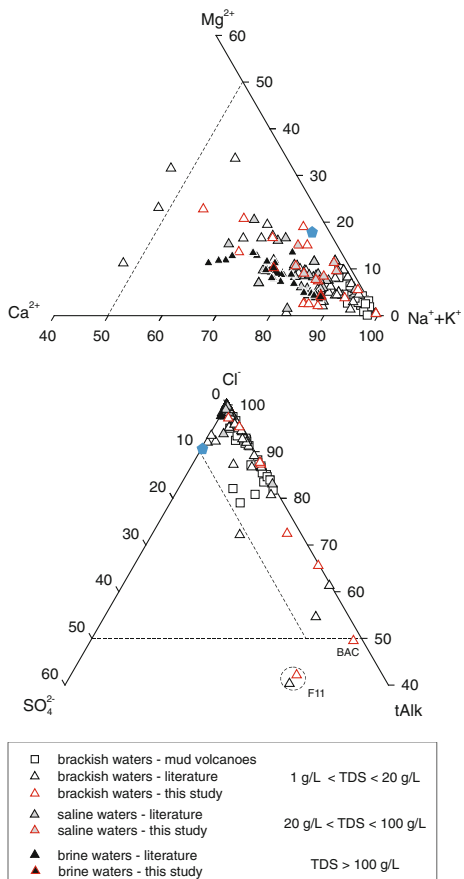
Table 2 continued

Code	$\delta^{18}\text{O}(\text{H}_2\text{O})_{\text{c}}$ ‰ vs. V-SMOW	$\delta^{18}\text{O}(\text{H}_2\text{O})_{\text{a}}$ ‰ vs. V-SMOW	$10^3 \ln \Gamma$	$\text{O}$	$\delta^2\text{H}(\text{H}_2\text{O})_{\text{c}}$ ‰ vs. V-SMOW	$\delta^2\text{H}(\text{H}_2\text{O})_{\text{a}}$ ‰ vs. V-SMOW	$10^3 \ln \Gamma$	$\text{H}$	$\delta^{37}\text{Cl}$ ‰ vs. SMOC	$\delta^{38}\text{Br}$ ‰ vs. SMOB	$^{87}\text{Sr}/^{86}\text{Sr}$	$\delta^{34}\text{S}(\text{SO}_4)$ ‰ vs. V-CDT	$\delta^{18}\text{O}(\text{SO}_4)$ ‰ vs. V-SMOW
<i>Saline waters</i>													
ISA1	-6.62	-6.66	-0.04	-45.3	-44.4	0.9	-0.31	-0.32	0.70881	-	-	-	-
RIT1	-1.34	-1.39	-0.04	-7.1	-6.0	1.1	-0.38	-0.08	0.70899	-	-	-	-
CSP1	0.01	-0.03	-0.04	0.6	1.8	1.2	-0.82	-0.15	0.70884	-	-	-	-
CSP2	-7.14	-7.18	-0.04	-49.0	-47.7	1.3	-	-	-	-	-	-	-
CC1	-3.33	-3.38	-0.05	-27.2	-25.5	1.7	-0.56	0.83	0.70898	-	-	-	-
BRI1	-4.07	-4.14	-0.07	-33.9	-32.1	1.8	-0.72	0.40	0.70894	-	-	-	-
SL13	-4.34	-4.44	-0.10	-30.3	-27.5	2.7	-0.03	0.37	0.70936	-	-	-	-
FRA2	-2.55	-2.63	-0.09	-22.8	-19.9	2.9	-	-	-	-	-	-	-
FRA2AS	-1.70	-1.77	-0.07	-16.5	-13.6	2.9	-	-	-	-	-	-	-
FRA1	-2.70	-2.80	-0.10	-24.4	-21.3	3.1	0.07	0.39	0.70905	-	-	-	-
<i>Brine waters</i>													
MONT1	-0.74	-0.93	-0.19	-11.6	-7.2	4.3	-0.01	-0.04	0.70898	-	-	-	-
SL4	0.48	0.35	-0.13	-7.4	-2.0	5.4	-0.03	0.17	0.70922	-	-	-	-
27SALMAG1	10.60	10.56	-0.04	-14.8	-9.4	5.4	0.18	0.44	0.70876	37.6	25.8	-	-
210SALMAG1	11.37	11.25	-0.12	-16.0	-10.4	5.6	0.31	0.26	0.70870	32.0	22.3	-	-

Isotope composition of the water molecule  $\delta^2\text{H}(\text{H}_2\text{O})\text{-c}$  and  $\delta^{18}\text{O}(\text{H}_2\text{O})\text{-c}$  was measured after distillation-condensation of the whole sample, whereas isotope activities  $\delta^2\text{H}(\text{H}_2\text{O})\text{-a}$  and  $\delta^{18}\text{O}(\text{H}_2\text{O})\text{-a}$  were estimated after calculation of the isotope salt effect by  $\text{EQ3/6}: 10^3 \ln \Gamma = \sum m_i (a_i + b_i/T)$  where  $m$  = molality,  $T$  = temperature (K),  $i$  is the  $i$ th salt and  $a_i$  (molality $^{-1}$ ) and  $b_i$  ( $\text{K} \times \text{molality}^{-1}$ ) experimental parameters for NaCl, KCl, MgCl<sub>2</sub>, CaCl<sub>2</sub>, Na<sub>2</sub>SO<sub>4</sub>, MgSO<sub>4</sub> listed in Horita et al. (1993)

“—” Not analyzed or not calculated

**Fig. 2** Ca–Mg–(Na + K) and SO<sub>4</sub>–Cl–tAlk (total alkalinity) (Equivalent/L) ternary classification diagrams of the salt waters from Northern Apennine and its foredeep. Data from this study (Table 1) and literature (Appendix 1 in Electronic supplementary material). Pentagon represents the mean chemical composition of the present-day seawater



data of this study are compared with 156 salt water analyses of the Po Plain from the literature (Appendix 1 in Electronic supplementary material), the role of seawater in the origin of the investigated waters is well supported: in the diagram Na–Cl, brines and saline waters plot close the seawater evaporation path (Fontes and Matray 1993) with the MONT and SALMAG brines located between the points of gypsum and halite precipitation. As occurring in the interstitial waters of the drilled Miocene sediments of the W-Mediterranean floor (Provence Basin, Vengosh et al. 1994) and elsewhere (Bein and Dutton 1993; Rosenthal 1997 and references therein), in the investigated samples the Na/Cl mol ratio decreases from saline (average = 0.82; median = 0.83;  $N = 41$ ) to brine waters (average = median = 0.77;  $N = 44$ ). In the brackish waters from mud volcanoes and in samples F15, SALV, MGR and BAC, the Na/Cl ratio is higher than unity. For MGR and BAC, which have low TDS, the ratio higher than 2 is due to mixing with Na-carbonate water (see sample F11 in Fig. 3; Venturelli et al. 2003; Iacumin et al. 2007). The investigated brackish waters have Na/Cl in the range 0.68–1.40, thus they cannot be interpreted as generated by simple mixing between marine water (Na/Cl = 0.85, atomic ratio) or via dissolution of halite (Na/Cl = 1). Diagrams of Cl vs. other halogens may be useful to investigate the characters of the saline component. For instance, Br has a conservative

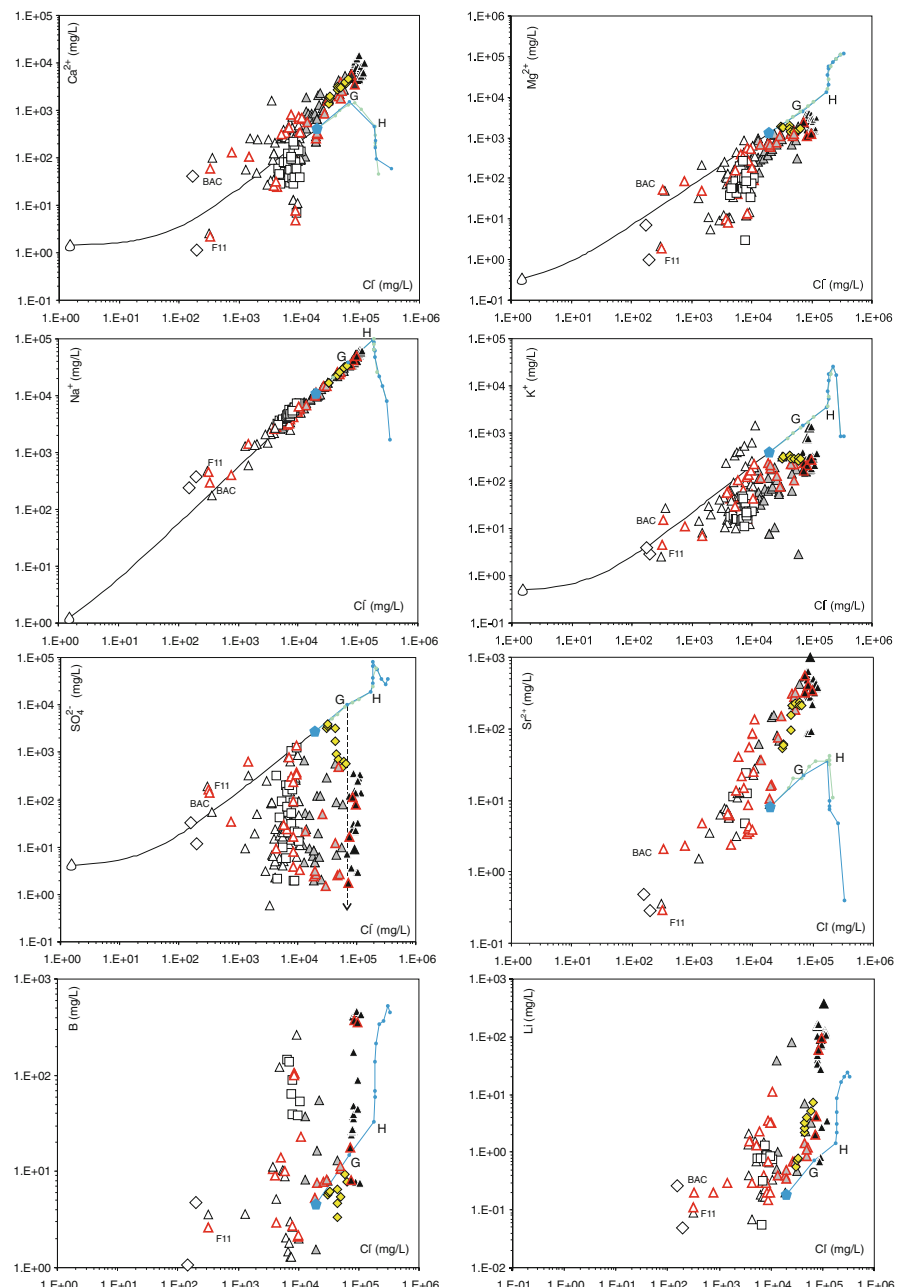


**Fig. 3** Chlorine vs. other elements logarithmic plots for the salt waters from Northern Apennine Foredeep (symbols as in Fig. 2; open diamonds: Na-bicarbonate waters from the Po Basin, Venturelli et al. 2003). Data from this study and the literature (Appendix 1 in Electronic supplementary material) are compared with Miocene interstitial waters from the W-Mediterranean (closed diamonds; Vengosh et al. 1994), the evaporation trajectory of seawater (circles: data from Fontes and Matray 1993, and Pierre 1982; G and H: gypsum and halite precipitation point) and seawater–meteoric water mixing line (drop: present-day meteoric water, data from Venturelli 2003)

behavior during evaporation of seawater and low partition coefficient in halite (Siemann and Schramm 2000), thus water dissolving halite (or other evaporitic chlorides) leads to Br/Cl ratio lower than in seawater ( $\text{Br}/\text{Cl} = 1.52 \times 10^{-3}$ ).

In Fig. 4, updated from Toscani et al. (2007), the samples in study are compared with data from the literature. Waters of meteoric origin interacting with Mesozoic carbonates and evaporites of the Tuscany and Emilia slope of Northern Apennine changed the early Ca-bicarbonate composition into Ca–SO<sub>4</sub> or Na–Cl types by dissolution of gypsum/anhydrite or halite, respectively (data from Bencini et al. 1977; Boschetti et al. 2005; Cortecci et al. 2008 and our unpublished). Some of these waters plot close the mixing lines connecting bicarbonate waters and halite saturated marine waters. Other samples (F15, BOB, SALMIN, BERG, PM) exhibit lower Br/Cl ratio ( $0.13 \times 10^{-3}$  to  $0.41 \times 10^{-3}$ ) and trend toward the field of waters with large amount of dissolved halite, thus supporting an important role of dissolution of Triassic evaporitic minerals in their evolution. Effectively, these springs outpour in Tuscany (SW slope of the Northern Apennine) or from geological unit of the Tuscan nappe (e.g. Bobbio window, Molli 2008) where Triassic evaporites occur.

Many brines plot between gypsum and halite precipitation points. The elevated concentrations of bromine and, especially, iodine in some saline and brine waters were explained by decomposition of organic matter in the sea (Toscani et al. 2007). It is noteworthy that the range of iodine contents in saline and brine waters of the Po plain is comparable with that found in pore waters of the Peruvian margin (Martin et al. 1993), an area where organic matter decomposition is very active. Due to the penesaline paleoenvironment, toxic for most marine organisms, and the low redox conditions at depth after burial, also brine waters of the sedimentary basins reach extremely high iodine contents similar to pore waters in convergent margin (~140 mg/L).

In the other element vs. Cl diagrams (Fig. 3), the investigated saline and brine waters plot far from the seawater evaporation path: the higher Ca, Sr, Li and B and the lower Mg, K and SO<sub>4</sub> contents support interaction with sediments during early-to-late diagenesis and redox processes. In the Cl–SO<sub>4</sub> diagram, the sulfate content of the waters is trending down the seawater evaporation line. In particular, the W-Mediterranean interstitial waters with the lowest sulfate contents plot close to the most sulfate saline and brine waters of the Po Basin (Figs. 3, 4). This is the product of sulfur loss due to sulfate reduction in an aerobic environment, which is typical of marine pore waters during early (Provence Basin) and late (Po Basin) diagenesis (e.g. van der Weijden 1992).

The measured isotope composition ( $\delta$ ) and calculated “activity” ( $\delta a$ ) for hydrogen and oxygen (Fig. 7) in the water molecule of the investigated waters are reported in Table 2. The brackish waters with lower salinity have meteoric imprint: actually, they plot toward the values of the present-day local ground and river waters ( $-10.3\text{\textperthousand} < \delta^{18}\text{O} < -7.1\text{\textperthousand}$ ,  $-45.2\text{\textperthousand} < \delta^2\text{H} < -72.2\text{\textperthousand}$ ; Iacumin et al. 2009). At increasing salinity, two features are noteworthy: (1) salt effect is relevant for the hydrogen isotope values of saline and brine waters (2) chlorine and bromine isotope values of brines are quite similar to seawater standard (0‰). Moreover, the brines MONT, SL4, SALMAG and the brackish water SALV, characterized by slightly negative  $\delta^2\text{Hc}$  values ( $-16.0$  to  $-7.4\text{\textperthousand}$ ), show a moderate to extreme shift toward highly positive  $\delta^{18}\text{Oc}$  values (up to  $+11.4\text{\textperthousand}$  for SALMAG), suggesting that the early isotopic composition of the waters was modified by high temperature interaction with the rocks (e.g. Fig. 1 in Horita 2009).

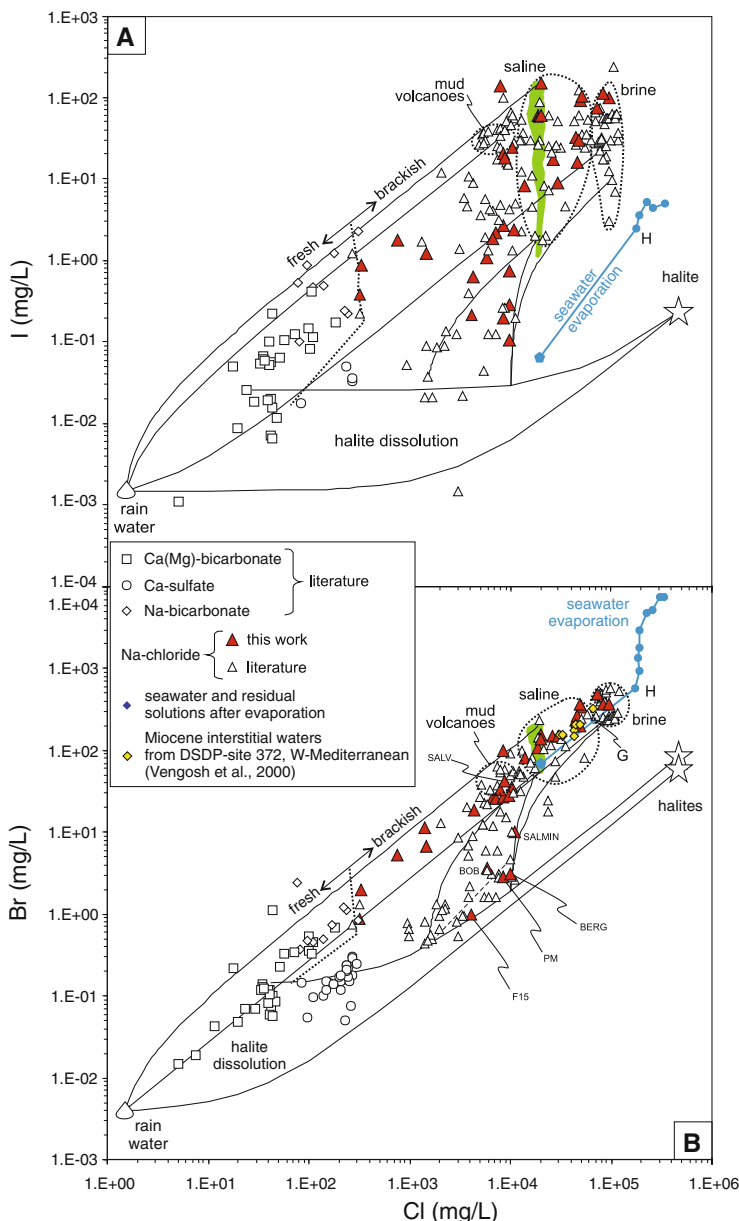


**Fig. 4** Chlorine vs. iodine (**a**) and bromine (**b**) logarithmic plots for waters from Northern Apennine and its foredeep, updated from Toscani et al. (2007). Data from this study and the literature (Appendix 1 in Electronic supplementary material; Agip Mineraria 1959) are compared with Miocene interstitial waters from the W-Mediterranean (**B**, closed diamonds; Vengosh et al. 2000), the evaporation trajectory of seawater (Fontes and Matray 1993, G and H: gypsum and halite precipitation point) and hypothetical binary mixings or halite dissolution (continuous lines). Shaded area collects present-day pore waters of oceanic sediments with active organic matter decomposition (Martin et al. 1993)

## 5 Discussion

### 5.1 Ca–Cl–Na Relation and Cationic Composition Activity Diagrams: Tracing Diagenetic Effects

Ca–Cl waters are distributed worldwide, but common geochemical parameters cannot discern the different processes producing this type of water (Rosenthal 1997). Secondary processes occurring after seawater evaporation and during the diagenetic evolution of basinal fluids may be identified with difficulty in binary plot. The plot of Davisson and Criss (1996) overcomes this inability using the two parameters  $\text{Na}_{\text{deficit}}$  and  $\text{Ca}_{\text{excess}}$  (mEq/L) which are defined as follows:

$$\begin{aligned}\text{Ca}_{\text{excess}} &= 2[\text{Ca}_{\text{meas}} - (\text{Ca}/\text{Cl})_{\text{SW}} \times \text{Cl}_{\text{meas}}]/40.08 \\ \text{Na}_{\text{deficit}} &= [(\text{Na}/\text{Cl})_{\text{SW}} \times \text{Cl}_{\text{meas}} - \text{Na}_{\text{meas}}]/22.99\end{aligned}$$

where  $\text{meas}$  = sample concentration; SW = seawater. In the Davisson and Criss' plot the Basinal Fluid Line (BFL), obtained by linear regression of more than 800 samples from several fluid reservoirs, represents the effect of plagioclase albitionization on water composition ( $\text{Na}/\text{Ca} = 2/1$  atoms). Figure 5a shows that the distribution of brines plot between BFL and a parallel line with negative intercept on the  $\text{Ca}_{\text{excess}}$  axis. It is noteworthy that this latter line crosses the seawater evaporation line in the middle of the path connecting gypsum and halite evaporation points. Historical data for SALMAG and FRA brines plot on BFL, whereas our samples, with other brines, are shifted toward the second line.

In particular, the Tolentino waters (SL samples in Table 1) define a wide area which reaches high  $\text{Ca}_{\text{excess}}$  and  $\text{Na}_{\text{deficit}}$  values. That suggests that feldspar albitionization is a predominant reaction in the sediment of the aquifer. According to Davisson and Criss (1996), dolomitization leads to high  $\text{Ca}_{\text{excess}}$  (Fig. 5a); for instance, in the samples with  $\text{Na}_{\text{deficit}} = 0$  and high  $\text{Ca}_{\text{excess}}$  up to intercept BFL line, dolomitization was strong (SALMAG), whereas it was lower for some brackish (BERG, SALMIN) and saline waters (e.g. CC samples, Fig. 5b). It is noteworthy that brine waters from localities not far one from the other (e.g. SALMAG, Cortemaggiore, Fontevivo) show different degrees of dolomitization–albitization, whereas brackish and saline waters plot around the origin of the axes like seawater or water with similar  $\text{Ca}_{\text{excess}}\text{–Na}_{\text{deficit}}$  values, confirming that dolomitization and albitization played a minimal control at these sites. Due to the slightly negative  $\text{Ca}_{\text{excess}}$  ( $\approx -10$ ) and highly negative  $\text{Na}_{\text{deficit}}$  ( $\approx -100$ ), the SALV water represents an exception (Fig. 5b). This water and the brackish waters from mud volcanoes depict a trend from seawater toward negative values of both variables. In this case, probably Na derives from clay dewatering at overpressure conditions (Xie et al. 2003) and/or albite dissolution (high pH).

In spite of the uncertainty of the field limits in the activity diagrams, the investigated brines plot prevalently within the stability field of low temperature albite and near or along the boundary with diagenetic zeolites (Fig. 6a1, a2). Actually, heulandite-clinoptilolite occur in the arenaceous formations of the Northern Apennines. In particular, heulandite is stable at high silica activity (near the amorphous silica saturation), i.e. far from the conditions of our brines. For silica activity ranging from  $\log \text{SiO}_2 = -3.5$  to cristobalite saturation, the Po Basin brines cluster along the low\_albite-mesolite and low\_albite-clinoptilolite\_  $\text{Ca}^{2+}$  limits (Fig. 6a1, a2), respectively, suggesting that only a partial albitization of the anorthitic plagioclase occurred. This does not contradict the supposed origin of the Basinal Fluid Line (Fig. 5). Actually, the following reactions of anorthite zeolitization

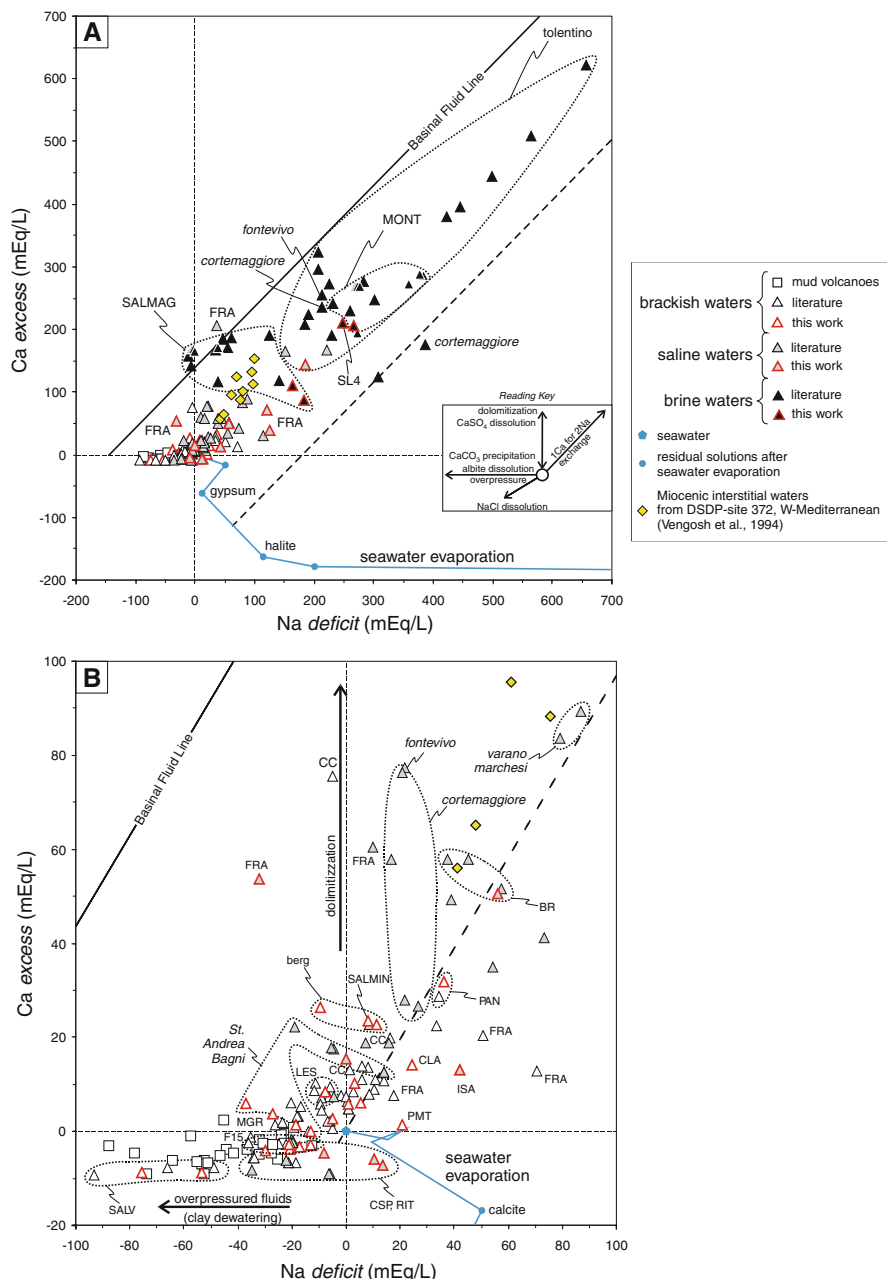
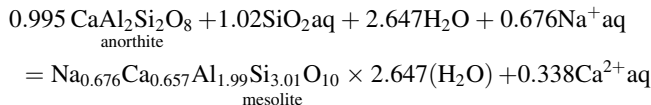
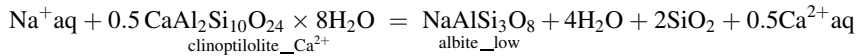
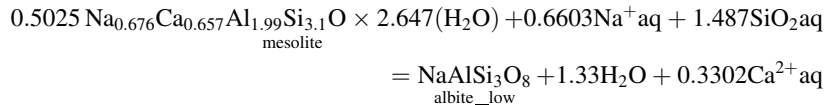


**Fig. 5** **a**  $\text{Na}_{\text{deficit}}$  vs.  $\text{Ca}_{\text{excess}}$  diagram for salt waters from the Northern Apennine Foredeep (symbols as in Fig. 2; data from this study and the literature—Appendix 1 in Electronic supplementary material). The basinal fluid line (BFL, Davisson and Criss 1996) represents the average global trend for high salinity fluids in deep continental environments that is similar to a 1Ca–2Na exchange line during albitionization. Dashed line parallel to BFL defines albitionization starting after seawater evaporation. Evaporation trend of seawater (data from Fontes and Matray 1993) and pore waters from the W-Mediterranean (diamonds; Vengosh et al. 1994) is also reported for comparison. **b** detail of (a)



and zeolite albitization



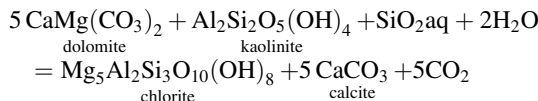
with 2Na–1Ca ratio suggest that exchange processes involving zeolites may also concur to generate the Basin Fluid Line.

In sedimentary basins, illite is involved in reactions which are relevant for diagenesis: (1) the releases of water during transformation of early kaolinite and smectite (clay dehydration); (2) the potassium and silica budget. In the Cortemaggiore field, formation waters were supposed to be in equilibrium with clays and, in particular, with illite at high K<sup>+</sup>/H<sup>+</sup> ratio of the interstitial fluids (Long and Neglia 1968). This hypothesis is confirmed by the specific activity diagram (Fig. 6b, c), where brine samples are clustered at the (K-feldspar)-kaolinite-montmorillonite-illite stability fields. The imperfect match of samples with the mineral stability fields and limits is probably due to several causes as the kinetic and pressure effects at low temperature, the chemical composition of the minerals (solid solution between Na–Ca–Mg–K bearing phases) and/or the possible dilution of the brines by freshwater during eogenesis or telogenesis. Also the reactions between calcite, illite (or mica s.s.) and K<sup>+</sup> to form K-feldspar could be involved in brine evolution; for instance (Carpenter 1978):

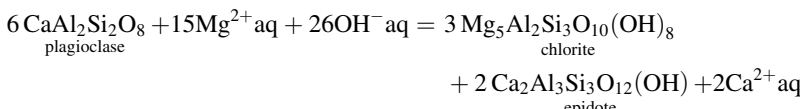


In Fig. 6c, the cristobalite-β stability field matches neither our samples nor the stability field of illite, so we can infer that quartz buffers silica in water and favors the nucleation of illite.

The chlorite formation during burial diagenesis is another important process often overlooked that, similarly to dolomitization, leads to Ca-increase and Mg-decrease in water. Chlorite can form by the following reactions involving kaolinite and dolomite during late diagenesis (Hutcheon 2002)



or anorthite chloritization–epidotization



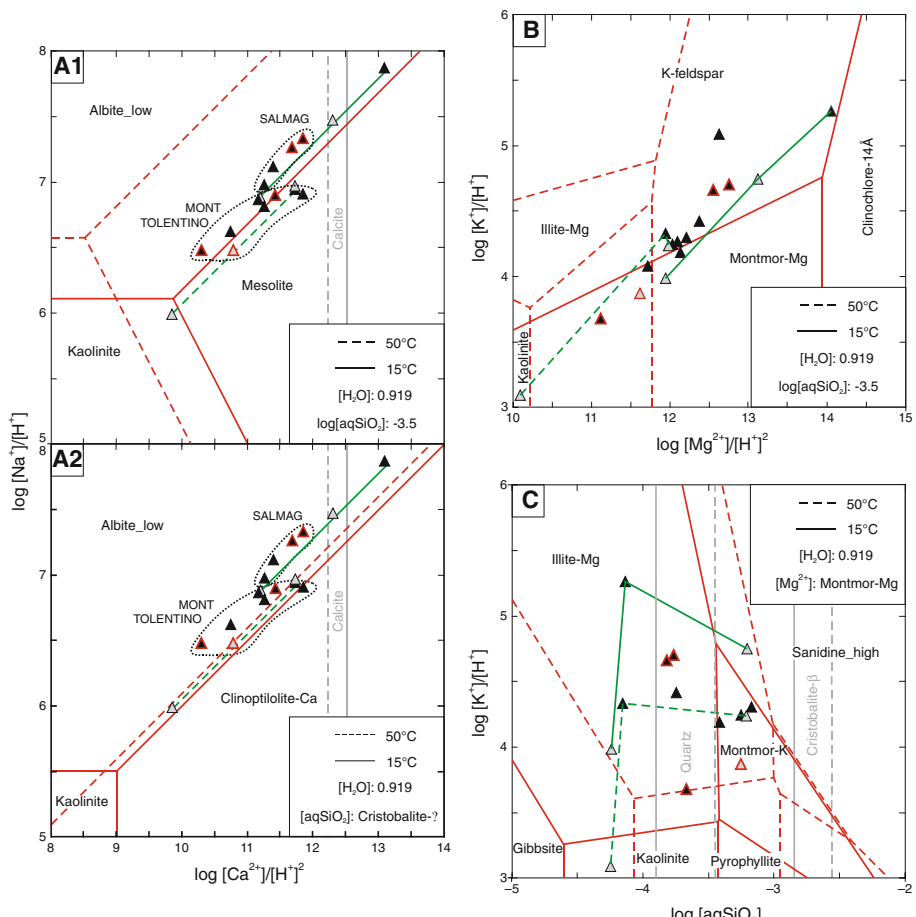


**Fig. 6** Activity plots for  $\text{Na}_2\text{O}-\text{CaO}-\text{SiO}_2-\text{Al}_2\text{O}_3-\text{H}_2\text{O}$  (A1 and A2),  $\text{K}_2\text{O}-\text{MgO}-\text{SiO}_2-\text{Al}_2\text{O}_3-\text{H}_2\text{O}$  (B) and  $\text{K}_2\text{O}-\text{SiO}_2-\text{Al}_2\text{O}_3-\text{H}_2\text{O}$  (C) systems at  $P = 1$  bar, 15°C (solid lines) and 50°C (dashed lines),  $\text{Al}_2\text{O}_3$  buffered with kaolinite (A1, A2, B, C),  $\text{SiO}_2$  with cristobalite- $\beta$  (A2) and MgO with montmorillonite-Mg(C). Solute activities of some representative saline (gray triangles) and brine (black triangles) water samples from Salsomaggiore, Monticelli and Tolentino were calculated by EQ3/6 code with Pitzer database at 15°C (red rims: samples from this study). In order to show the temperature effect, the activities of the Cortemaggiore field samples were calculated at 15°C (solid line link) and at 50°C (dashed line link). The solubility limits of calcite (A1, A2), quartz and cristobalite- $\beta$  (C) are referred to a mean local brines with  $\text{Cl} = \text{Na} = 2.968 \text{ mol/L}$  and  $\log P(\text{CO}_2) = -2.72$

The activity diagram of Fig. 6b shows that the chlorite field (clinochlore-14 Å) expands toward lower  $\text{Mg}^{2+}/(\text{H}^+)^2$  values at higher temperature in similar way to Po Plain brines.

In summary, the activity diagrams indicate that burial diagenesis and related water–rock interaction modified the original Ca, Na and K contents of the evaporated seawater and influenced the lithology of the host aquifer. For the waters studied, both dolomitization and Ca–Na exchange reactions (zeolitization–albitization) occurred in the foredeep basins: the former was dominant at Salsomaggiore (SALMAG), whereas the latter dominated at Tolentino. The role of clay minerals is multiform: dewatering at overpressure conditions, leading to the formation of Na-rich brackish waters (SALV and mud volcanoes), to

illitization–chloritization in brines. Considering that strontium replaces calcium in feldspar; in the next paragraphs we will consider the  $^{87}\text{Sr}/^{86}\text{Sr}$  isotopic ratio in the aqueous phase as indicator of water–rock interaction.

## 5.2 Geothermometry

The application of chemical geothermometers to formation waters can be inadequate because the P- and T variations, during the geological evolution (e.g. burial diagenesis), may change the original physical–chemical conditions of the waters. In the limits of this consideration, empirical relations, such as Mg–Li and to some extent the Na–Li geothermometers (Kharaka and Mariner 1989) are considered to be more successful than equilibrium relations (Land and Macpherson 1992) in predicting the subsurface temperatures of brine waters in sedimentary basins. For the SALMAG brines, the average temperature evaluated by Mg–Li geothermometer is  $156 \pm 15^\circ\text{C}$  (mean  $\pm$  SD;  $N = 12$ ). This value does not differ significantly from  $170 \pm 18^\circ\text{C}$  (mean  $\pm$  SD;  $N = 12$ ) obtained by Na–Li and is comparable to  $145 \pm 23^\circ\text{C}$  (mean  $\pm$  SD;  $N = 2$ ) obtained by  $\text{SO}_4\text{-H}_2\text{O}$  oxygen isotope geothermometry (Seal et al. 2000).

Compared to Mg–Li and Na–Li empirical geothermometry, silica geothermometers give lower temperature. This discrepancy is probably due to the control exerted by quartz or other silica phases on dissolved silica species during early equilibration at depth (e.g. silica buffer during illitization and zeolitization) and/or later during water migration in the aquifer. Chalcedony and quartz geothermometers (corrected for activity and pressure; Kharaka and Mariner 1989) applied to the Salsomaggiore and Cortemaggiore data give  $58\text{--}77^\circ\text{C}$  and  $89\text{--}106^\circ\text{C}$ , respectively. Considering the present-day mean geothermal gradient of  $30^\circ\text{C/km}$  and the cross-section of the area (Fig. 1b and Pieri 1992), the values obtained by silica geothermometers are between the temperature at the borehole depth (down to 2.5 km; last silica equilibrium) and the depth of the Marnoso-Arenacea over-thrust (down to 3.5 km; early silica equilibrium). As the Salsomaggiore brine is thought to be responsible for dolomite formation in the sediment of the aquifer, we applied also the calcite/dolomite geothermometer of Hyeong and Capuano (2001) using the  $\text{Ca}^{2+}$  and  $\text{Mg}^{2+}$  calculated by EQ3/6 software (supposing the calcite/dolomite equilibrium) and YPF database (Pitzer) at the outpouring temperature of  $16^\circ\text{C}$ . At these conditions, however, the geothermometer with equation

$$\log(a\text{Ca}^{2+}/a\text{Mg}^{2+}) = [(7.21 \times T)/1000] - 0.22$$

is scanty because of the resulting negative temperature ( $\log(a\text{Ca}^{2+}/a\text{Mg}^{2+}) = -0.46$  to  $-0.78$ ). Taking into account the temperatures obtained by other geothermometers, we recalculated the activities of  $\text{Ca}^{2+}$  and  $\text{Mg}^{2+}$  at  $150^\circ\text{C}$  obtaining  $\log(a\text{Ca}^{2+}/a\text{Mg}^{2+})$  from 0.645 to 0.703, which gives a temperature range of  $120\text{--}128^\circ\text{C}$ . Once more, these results unfit. Nonetheless, if we apply the obtained  $\text{Ca}^{2+}$  and  $\text{Mg}^{2+}$  activity ratio to the equilibrium between calcite and disordered dolomite



and using the  $\log K$  polynomial fit calculated for  $0\text{--}300^\circ\text{C}$  temperature range

$$\begin{aligned} \log(a\text{Ca}^{2+}/a\text{Mg}^{2+}) &= \log K = -0.6954 + (0.01465 \times T) - [(5.33e - 5) \times T^2] \\ &\quad + [(1.16e - 7) \times T^3] - [(1.086e - 10) \times T^4] \end{aligned}$$

we obtain the temperature interval of  $151\text{--}163^\circ\text{C}$ .

Chemical and geothermometric data suggest that the aquifer containing the brine of Salsomaggiore underwent dolomitization at relatively high temperature. As the aquifer of Salsomaggiore evolved in a sedimentary environment, we have to suppose that the calculated mean temperature of 150°C is explained by the geological evolution for burial down to 5.0–7.5 km depth. It is noteworthy the calculated range of depth corresponds to the sources of gas and oil in the area (Pieri 1992, 2001) and, considering a geothermal gradient of 20°C/km, to depth of fresh sediments (Cataldi et al. 1995; Wygrala 1987; Pieri 2001). The present-day depth of the Salsomaggiore reservoir is shallower than in the intra-Messinian orogenic phase because of the exhumation of the structure after early burial (Artoni et al. 2004, 2007).

### 5.3 Oxygen and Hydrogen Isotope Composition of Water

Explanations for the stable isotope systematics of basinal brines are peculiar for each basin, but some features, such as the involvement of meteoric water and evolved marine component, are common to brines from all basins (Sharp 2007). However, isotope composition of ancient water end-members is difficult to know, in particular for the residual evaporated seawater, the value of which depends on the initial isotopic and chemical composition of ancient seawater and on relative air humidity of the paleo atmosphere. The water of the hydrated saline minerals is useful to overcome this problem, since it can be used to obtain the isotopic composition of the mother solutions that precipitated the evaporitic minerals. As inferred from chemistry (Figs. 2, 3), the studied brine waters represent the composition of evaporated seawater near the gypsum precipitation point, and the isotopic composition of mother water of Messinian gypsum would be a consistent end-member. Scanty data on the isotope composition of the Po Basin Messinian gypsum mother water were published (“Vena del Gesso” formation; Longinelli and Ricchiuto 1977), whereas for the coeval “Gessoso-Solfifera” formation of Sicily plentiful and complete data sets are available (Pierre and Catalano 1976; Censi 1984; Bellia and Censi 1985; Bellanca and Neri 1986). In Fig. 7, the gypsum mother waters plot in two separate fields: (1) waters affected by burial diagenesis showing higher  $\delta^{18}\text{O}$  and lower  $\delta^2\text{H}$  values (Censi 1986) and with a  $^{18}\text{O}$ -shift similar to some salt waters (e.g. Fontevivo and SALV samples); (2) waters unaffected by diagenesis showing a rough triangular distribution connecting the evaporating mother-seawater at the stage of gypsum precipitation and the meteoric water lines (GMWL and MMWL). The observed distribution probably reflects the composition of the palaeo seawater and the mixing with inflowing palaeo meteoric waters typical of regions with high air temperature, which is a Messinian meteoric water of  $\delta^2\text{H} \approx -5$  to  $-10\text{\textperthousand}$  and  $\delta^{18}\text{O} \approx -3$  to  $-5\text{\textperthousand}$ . It is noteworthy that the present-day isotope composition of the southeast portion of the Adriatic sea is within these values; this may be explained by the warm climatic conditions of the eastern Mediterranean region (Dolenec et al. 1996).

The waters geographically located eastward of Bologna, where the “Vena del gesso” formation outcrops (FRA, CC, BR, CSV, SER), define nearly straight line that could be related to mixing of two end-members represented, respectively, by the present-day river water, located on the local meteoric water lines (niwl and ciwl in Fig. 7; Longinelli and Selmo 2003) and the gypsum mother water similar to the present-day evaporated seawater at the point of gypsum precipitation (e.g. Pierre 1982). When we compare the stable isotope ratios for the waters and the chloride content (Fig. 8), this mixing can still be invoked for samples from “Vena del Gesso” formation, but the presence of a single saline

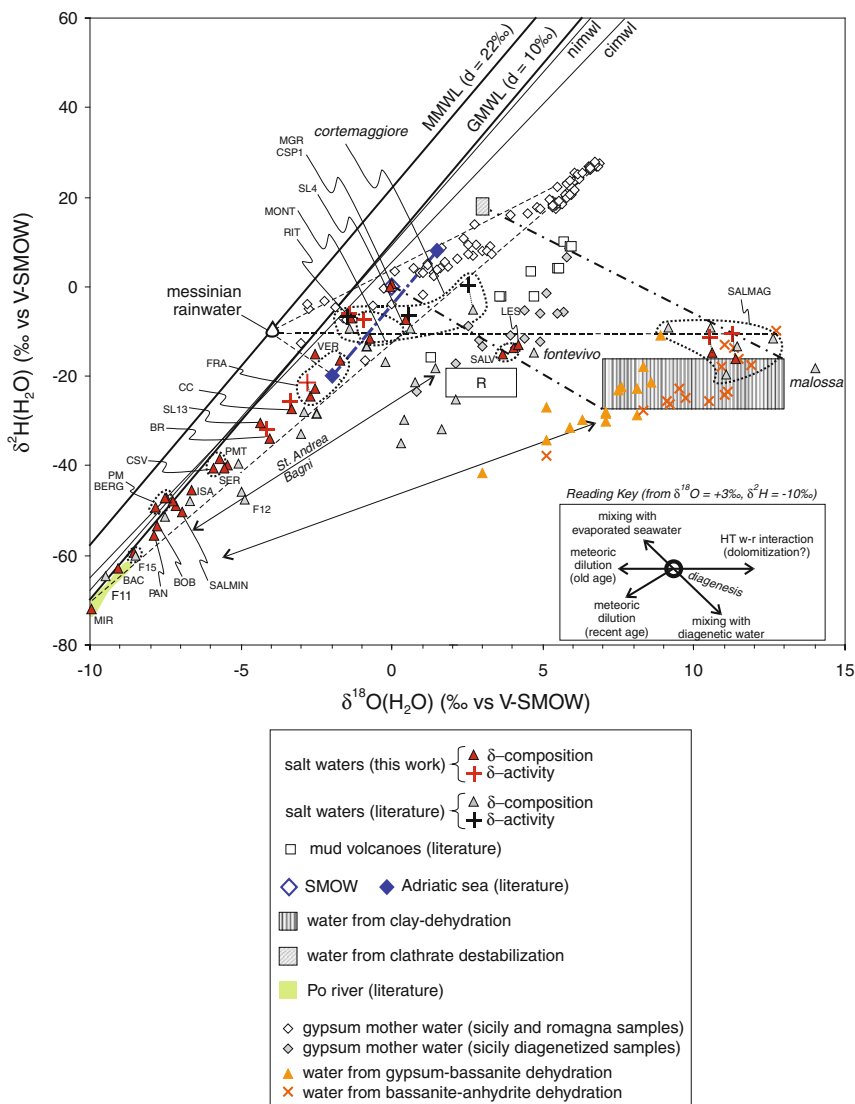


**Fig. 7**  $\delta^{18}\text{O}(\text{H}_2\text{O})$  vs.  $\delta^2\text{H}(\text{H}_2\text{O})$  values for the salt waters from Northern Apennines and related foredeep. GMML: Global Meteoric Water Line (Rozanski et al. 1993), MMWL: Mediterranean Meteoric Water Line (Gat and Carmi 1970), nimwl and cimwl: northern and central Italy meteoric water lines (Longinelli and Selmo 2003). R: field of the Regnano mud volcano (Capozzi and Picotti 2002). Salt waters data from literature: Salsomaggiore (Picotti et al. 2007); Fontevivo (Toscani et al. 2007); St. Andrea Bagni (Toscani et al. 2001; Iacumin et al. 2007); Cortemaggiore, Malossa and other Po Basin salt waters (Ricchiuto et al. 1985). Mother water data from primary gypsum (see text for references), diagenetic sulfate minerals and water from gypsum-bassanite and gypsum-anhydrite dehydration are shown (Censi 1986). Present-day composition of the Adriatic Sea (Dolenec et al. 1996) and Po river (Iacumin et al. 2009) is also reported. Water from clathrate destabilization was calculated using a seawater composition of  $\delta^{18}\text{O}(\text{H}_2\text{O}) = \delta^2\text{H}(\text{H}_2\text{O}) = 0\text{\textperthousand}$  and the clathrate-water fractionation factors after Maekawa and Imai (2000). The clay-dehydration field was calculated assuming an isotopic composition of generic clay, in geopressured system, of +17 to +23‰ for  $\delta^{18}\text{O}$  and -39 to -28‰ for  $\delta^2\text{H}$  and a clay-water fractionation at temperature of 150°C (Dähmlmann and de Lange 2003; Hyeong and Capuano 2004), obtaining a fluid composition of +7 to +13‰ for  $\delta^{18}\text{O}$  and -16 to -27‰ for  $\delta^2\text{H}$

end-member is excluded. In fact, mixing lines passing through our samples connect the present-day continental water with different points on the seawater evaporation line (Pierre 1982). Waters like CSV, RIT, SER, PAN and PTM derive from dilution of early seawater that could be represented by the CSP1 water. In fact, six monthly samplings during 2007–2008 of the CSP well have verified that its water isotope composition is similar to the present-day seawater ( $\delta^{18}\text{O}_c = 0.17 \pm 0.22\text{\textperthousand}$ ,  $\delta^2\text{H}_c = -0.7 \pm 0.8\text{\textperthousand}$ ,  $N = 6$ ; unpublished data). Waters CC, BR and ISA represent a meteoric dilution of previously evaporated seawater at the stage of gypsum saturation, whereas those from Tolentino (SL) and Fratta (FRA) at a stage intermediate between gypsum and halite saturation (Fig. 8). In the same diagram, also the trend shown by Cortemaggiore and Salsomaggiore brines starts from an evaporated seawater, but probably the dilution involves the participation of different types of fresh water: Messinian meteoric water at Cortemaggiore and/or a diagenetic water at Salsomaggiore. The overlap of sulfate and clay dehydration waters suggests that the gypsum to anhydrite reaction and the smectite to illite reaction concur to generate a sole diagenetic end-member (Fig. 7 and caption). However, at Salsomaggiore the extreme  $^{18}\text{O}$ -shift ( $\delta^{18}\text{O}$  = from +9‰ to +13‰) due to high temperature water–rock interaction was able to hide the above processes. In fact, it is noteworthy that  $\delta^{18}\text{O}$  values between –5 to +5 and +5 to +12 are typical of formation waters from sandstone and carbonate reservoirs, respectively (Morad et al. 2003). Moreover, the presence of  $^{18}\text{O}$ -enriched formation waters up to +8‰ was inferred by the isotope analysis of carbonate cement in the Tertiary sandstones of the N-Apennine Foreland Basin (Milliken et al. 1998). The  $\delta^{18}\text{O}$  values of Salsomaggiore brines are very similar to those of the saline waters from the Mesozoic oilfield of Malossa (from +13 to +14‰; Ricchiuto et al. 1985) about 50 km north of Piacenza (Fig. 1). This resemblance on isotope composition probably induced Picotti et al. (2006) to support the origin of the Salsomaggiore (SALMAG) brines from the Late Triassic “Dolomia Principale”. Ultrafiltration was invoked by the authors to relate the isotopic composition of the Salsomaggiore brines to that of mud volcanoes of the Po Plain (Regnano, Province of Reggio Emilia) and their genesis to an oil–water migration from deep Mesozoic formation. In the literature, membrane filtration was frequently used as *deus ex machina* to explain the oxygen and hydrogen isotope composition of formation waters. Generally speaking, experiments on membrane filtration showed  $^{18}\text{O}$ – $^2\text{H}$  and solute enrichment of the residual solution and  $^{18}\text{O}$ – $^2\text{H}$  depleting of the passing ultrafiltrate (Coplen and Hanshaw 1973); more recently, experiments have given contradictory or inconclusive results (Longstaffe 2000 and references therein). The low salinity (22–23 g/L) and the position in the chlorine–water isotope plot (Fig. 8) of the Malossa waters do not support at all a genetic relation by ultrafiltration with the Salsomaggiore brines. The wide shift toward high  $\delta^{18}\text{O}$  values probably reflects similar processes of high temperature water–rock interaction with carbonates both for Malossa (155°C, Mattavelli and Margarucci 1992) and Salsomaggiore (150°C, see previous geothermometry section), but the different chlorine content suggests independent origin and diagenetic histories.

With regard to Po Basin mud volcanoes, their isotopic composition is quite variable but could be explained by mixing of three components like (1) evaporated seawater, (2) present-day meteoric water and (3) water from clay dehydration (Figs. 7, 8). This interpretation agrees with the adopted geochemical (Martinelli and Dadomo 2005) and geophysical (Bonini 2007) models of the Po Basin mud volcanoes that suggest the supply of fluids with suprathydrostatic or near-lithostatic pressures for the deep and superficial reservoirs, respectively. For SALV and mud volcanoes, in addition to chemical composition, also isotope ratios support their similar origin, although minor  $^2\text{H}$  enrichments of the Po Basin’s mud volcanoes waters could also be inherited by isotopic

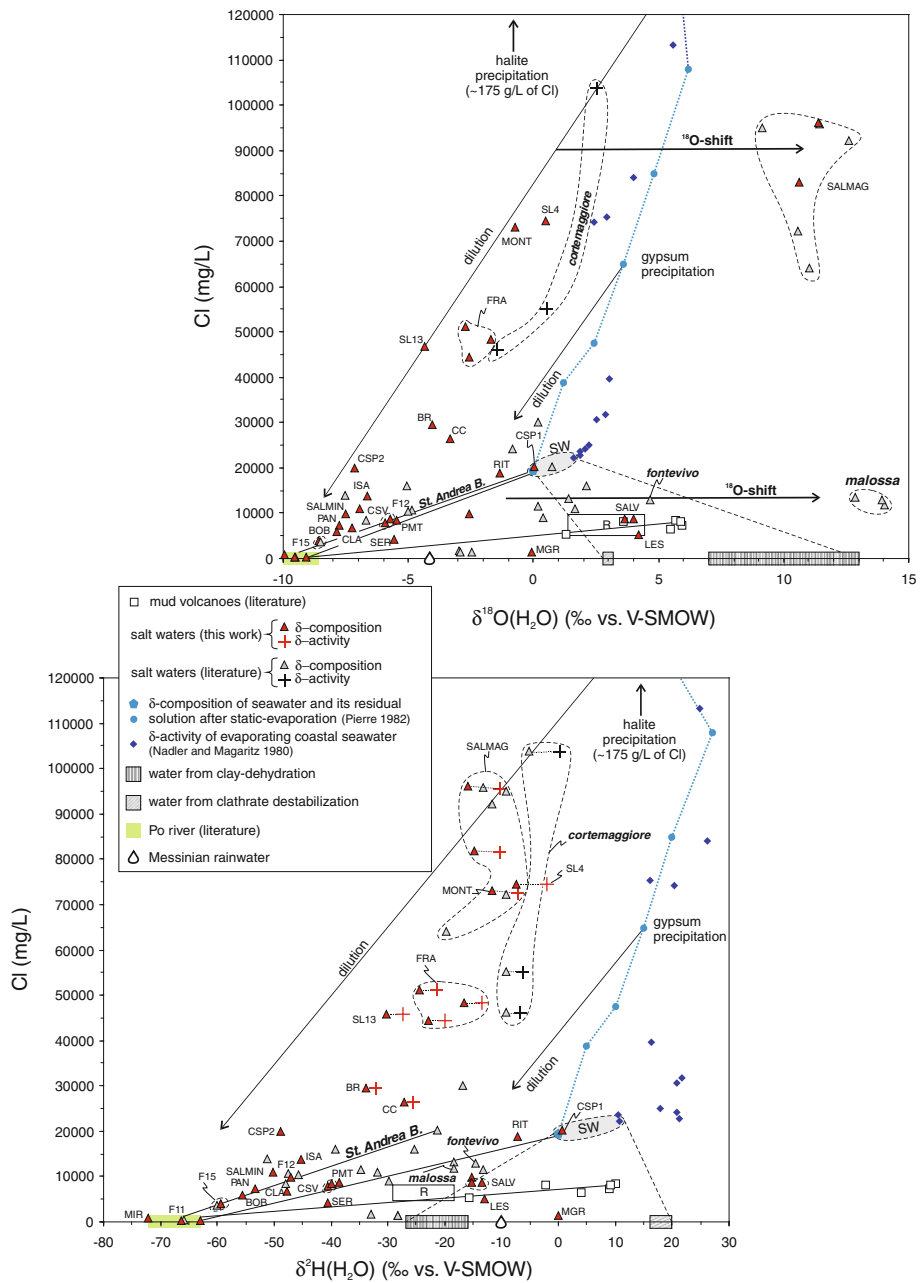


**Fig. 8** Chlorine vs.  $\delta^{18}\text{O}(\text{H}_2\text{O})$  and  $\delta^2\text{H}(\text{H}_2\text{O})$  diagrams for the salt waters from Northern Apennines and Po Basin; data from this study and literature (Capozzi and Picotti 2002; Iacumin et al. 2007; Picotti et al. 2007; Ricchiuto et al. 1985; Toscani et al. 2007). Waters from clay dehydration and clathrate ( $\text{Cl} \approx 0 \text{ mg/L}$ ) destabilization fields as in Fig. 7. SW: seawater

exchange with methane (e.g. Fig. 1 in Horita 2009). In this case, fresh water with enriched isotopic composition coming from destabilization of “ancient” gas-hydrates (Figs. 7, 8; Maekawa and Imai 2000; Conti et al. 2007) can be considered as a fourth component added by mixing.

#### 5.4 Sulfate Isotope Composition: $\delta^{34}\text{S}(\text{SO}_4)$ and $\delta^{18}\text{O}(\text{SO}_4)$

For the Salsomaggiore brines, in order to check their possible provenance from the Late Triassic formation, or its origin by mixing with waters coming from this formation, oxygen and sulfur isotope of sulfate molecule were compared with Messinian sulfate from the Mediterranean area (Longinelli 1979; Ricchiuto and McKenzie 1978; Pierre and Rouchy 1990; Lu and Meyers 2003), dissolved sulfate of Po Basin groundwaters interacting with Messinian sulfate (Olivero et al. 1987) and Triassic sulfate from Italian Eastern Alps (Longinelli and Flora 2007) and Northern Apennines (Boschetti et al. 2010; Fig. 9).

In the Po Basin, fresh to brackish groundwaters interacting with Messinian sulfates (Fig. 9, data from Olivero et al. 1987) depict an almost linear trend with a 0.38 slope “typical” of a kinetic fractionation (Fritz et al. 1989) or “intermediate” reduction rate (Brunner et al. 2005) starting near the “Messinian primary sulfate” ( $\delta^{34}\text{S} = +21.7\text{\textperthousand}$  and  $\delta^{18}\text{O} = +12.5\text{\textperthousand}$ ). This point was calculated considering the fractionation during gypsum precipitation from seawater (+1.65‰ for  $\delta^{34}\text{S}$ ; +3.5‰ for  $\delta^{18}\text{O}$ ; Thode and Monster 1965; Lloyd 1967) and assuming that  $\delta^{34}\text{S}$  and  $\delta^{18}\text{O}$  of marine dissolved sulfate are globally constant in space ( $\delta^{34}\text{S} = +20 \pm 0.5\text{\textperthousand}$ ;  $\delta^{18}\text{O} = +9.0 \pm 0.6\text{\textperthousand}$ ) and time, i.e. without significant change from Tertiary to present. However, the oxygen isotopic composition of buried and exposed Messinian sulfates vary considerably, reflecting the basinal environmental condition during sulfide oxidation. In particular, the  $^{18}\text{O}$ -enriched sulfate values between +17 and +20‰ are related to a “secondary sulfate” resulting from redox cycling in the deep basin where the oxygen is inherited from water (Lu et al. 2001). This is facilitated by a slow reduction rate which enables a more intense oxygen isotope exchange upon dissimilatory sulfate reduction reaction (Brunner et al. 2005). Sulfur isotope composition of the “Messinian secondary sulfate” is between +23.0 and +26.4‰ (Gavrieli et al. 1995; Böttcher et al. 1999), with a central value of +24.7‰ in accordance with +24.9‰ found in a Fontevivo saline water (Toscani et al. 2007). The back extrapolation line of the SALMAG samples intercepts the Messinian secondary sulfate field as well as the values of (Late) Triassic sulfate of the eastern Italian Alps. Thus, a significant involvement of a Triassic component cannot be excluded. However, it should be noted that pore waters interacting with Messinian sulfates recovered at depth during ODP drilling (Böttcher et al. 1998, 1999) in the western and eastern Mediterranean have a sulfate isotope composition similar to that of the SALMAG brines. Probably, these dissolved sulfates are residual sulfate from slowly reduced Miocene sulfate (inset in Fig. 9). Moreover, in the Po plain area near the Apennines, waters with Triassic-Messinian mixed sulfate such as Acqui Terme show a Triassic end-member of  $\delta^{34}\text{S} = +17.5\text{\textperthousand}$  and  $\delta^{18}\text{O} = +8.9\text{\textperthousand}$  (Olivero et al. 1987), comparable with the Northern Apennines mean values of  $\delta^{34}\text{S} = +15.2 \pm 0.3\text{\textperthousand}$  and  $\delta^{18}\text{O} = +10.9 \pm 0.5\text{\textperthousand}$  (Boschetti et al. 2010). Therefore, a Triassic origin for the SALMAG sulfate (and brine) is improbable.

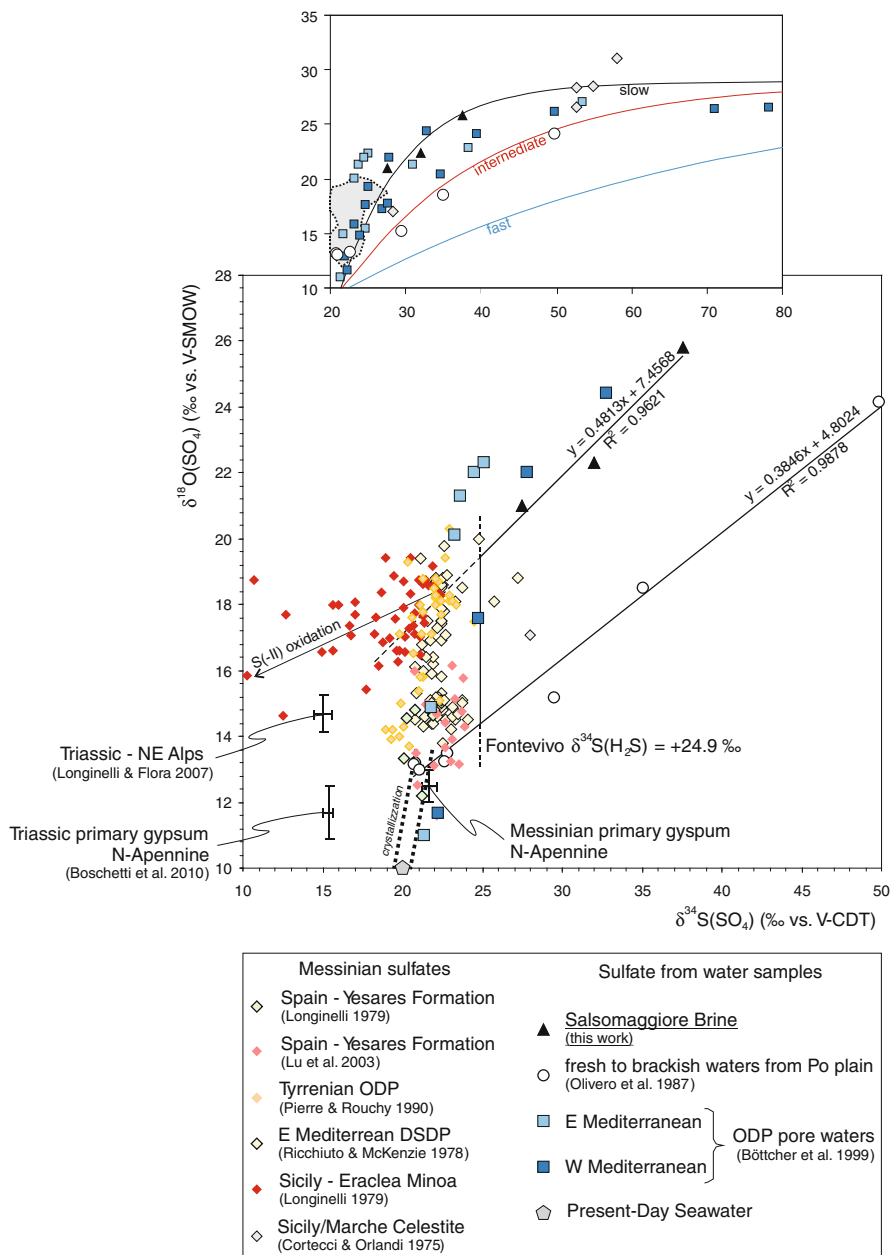


**Fig. 9**  $\delta^{18}\text{O}(\text{SO}_4)$  vs.  $\delta^{34}\text{S}(\text{SO}_4)$  relationship for Messinian sulfate minerals and dissolved sulfate in waters. Messinian primary sulfate is located at the top of the dotted crystallization path. Curves in the inset depict the evolution of residual sulfate in marine sediments at different reduction rate (Brunner et al. 2005). Values of sulfate minerals (diamond and gray field in the inset), brines (Salsomaggiore) and pore waters interacting with them are due to redox recycling in the ancient basin and/or slow reduction. Note that pore waters from Mediterranean interacting with Messinian sulfates (Böttcher et al. 1998, 1999) and Salsomaggiore brine data (this work) are placed on the slow reduction curve (inset). See text for details

### 5.5 Isotope Effects Induced by Thermochemical Sulfate Reduction

A complete thermochemical reduction of sulfate was supposed to explain the high measured value of  $\delta^{34}\text{S}(\text{H}_2\text{S}) = +24.9\text{\textperthousand}$  for the Fontevivo reservoir (Toscani et al. 2007). At the typical temperature of gas-souring reaction (140–150°C; Worden et al. 1996)



considering pure anhydrite and calcite, the  $\log K \cong \log (P_{\text{H}_2\text{S}}/P_{\text{CH}_4}) \cong +4.7$  (thermo.com.v8.r6 thermodynamic database; Hutcheon 2002). Thermodynamic recalculation of the chemical data of the Fontevivo brine at well bottom conditions gives  $\log (P_{\text{H}_2\text{S}}/P_{\text{CH}_4}) \cong +4.3$  (EQ3/6 software; Sborgi et al. 1936), which is slightly lower than the gas-souring equilibrium value.

At Salsomaggiore, H<sub>2</sub>S was never revealed but it is high in the neighboring area (e.g. Tabiano springs; Toscani et al. 2001). From the best-fit of  $\delta^{18}\text{O}(\text{SO}_4)$  and  $\delta^{34}\text{S}(\text{SO}_4)$  data of Salsomaggiore we obtain a  $\delta^{18}\text{O}(\text{SO}_4)$  value of  $+19.4\text{\textperthousand}$  for  $\delta^{34}\text{S}(\text{H}_2\text{S}) \equiv \delta^{34}\text{S}(\text{SO}_4) = +24.9\text{\textperthousand}$  of Fontevivo (Fig. 9).

Supposing that secondary Messinian anhydrite is the source of sulfate mineral for thermochemical sulfate reduction (TSR) and assuming that the oxygen isotopes of anhydrite are fractionated between calcite and water according to the above chemical reaction and the following equation (Worden et al. 1996)

$$\delta^{18}\text{O}(\text{H}_2\text{O}) = \delta^{18}\text{O}(\text{CaSO}_4) - 3/4 \times \Delta^{18}\text{O}_{\text{calcite}-\text{H}_2\text{O}(\text{l})}.$$

A resulting composition of  $\delta^{18}\text{O}(\text{H}_2\text{O}) = +9.9\text{\textperthousand}$  is calculated using the calcite-water fractionation at 150°C (O’Neil et al. 1969). Interestingly, this is similar to the oxygen isotope composition of the diagenetic water field (Fig. 7).

The same approach could be used to estimate the hydrogen isotope composition of the water obtained from the gas-souring reaction

$$\delta^2\text{H}(\text{H}_2\text{O}) = \delta^2\text{H}(\text{CH}_4) + 0.5 \times \Delta^2\text{H}_{\text{H}_2\text{O}(\text{l})-\text{H}_2\text{S}(\text{g})}$$

Due to the large hydrogen fractionation between water and hydrogen sulfide, it is misleading to represent  $\Delta\text{H}_{\text{H}_2\text{O}(\text{l})-\text{H}_2\text{S}(\text{g})}$  by the fractionation as  $10^3 \ln \alpha_{\text{H}_2\text{O}(\text{l})-\text{H}_2\text{S}(\text{g})}$  (e.g. Clark and Fritz 1997). However, considering the discrepancy between these values at 150°C,  $\Delta_{\text{H}_2\text{O}(\text{l})-\text{H}_2\text{S}(\text{g})} \cong 10^3 \ln \alpha_{\text{H}_2\text{O}(\text{l})-\text{H}_2\text{S}(\text{g})} - 138 \cong 438\text{\textperthousand}$  (Galley et al. 1972; Horita and Wesolowski 1994), and assuming  $\delta^2\text{H}(\text{CH}_4)$  from –150 to –180‰ for thermo-genic methane at Cortemaggiore and Salsomaggiore (Mattavelli et al. 1983; Borgia et al. 1988), we obtain  $\delta^2\text{H}(\text{H}_2\text{O}) \cong +69\text{\textperthousand}$  and +39, respectively. Apart from the large uncertainty of estimation, those high and unrevealed water hydrogen isotope values could suggest that (1) no gas-souring TSR occurs and bacterial reduction in a closed system explains the  $\delta^{34}\text{S}(\text{H}_2\text{S}) \equiv \delta^{34}\text{S}(\text{SO}_4)$ ; (2) methane is not the only major organic reactant because high percentage of crude oil and ethane exist in the hydro-carbon reservoir of the Parma Province (e.g. Borgia et al. 1988); (3) gas-souring reaction is more complicated and do not involve solid sulfate but only solution species and (4) the amount of released water is probably very small and negligible (Machel 2001; Hutcheon 2002).

### 5.6 Isotope Composition of Dissolved Halogens: $\delta^{81}\text{Br}$ and $\delta^{37}\text{Cl}$

The Cl and Br stable isotope values show wide variations for the sampled waters (Table 2; Fig. 10). However, the values of the brine waters of MONT, SL and SALMAG and the *quasi-brines* waters FRA plot close to standard mean ocean chloride (SMOC), whereas they are close to or enriched in comparison with standard mean ocean bromide (SMOB). Differently, SALV brackish water is highly enriched with  $^{81}\text{Br}$ .

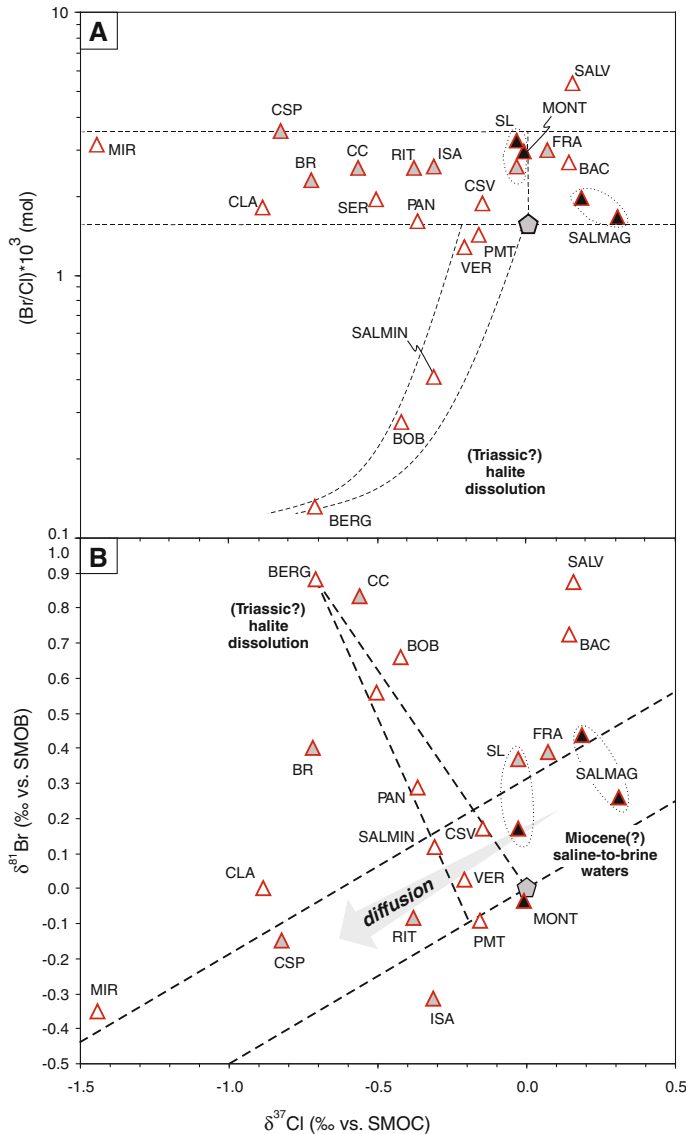


**Fig. 10**  $\delta^{37}\text{Cl}$  vs.  $\text{B}/\text{Cl}$  (a) and  $\delta^{37}\text{Cl}$  vs.  $\delta^{81}\text{Br}$  (b) relationships for the salt waters from Northern Apennines and its foredeep. Symbols as in Fig. 2

The variation of the chlorine isotope composition of Po plain salt waters is within, and indistinguishable from, the  $\pm 2\text{\textperthousand}$  global range of waters from sedimentary basins-oil fields (Fig. 3 in Stewart and Spivack 2004). However, when the  $\delta^{37}\text{Cl}$  values are plotted against the Br/Cl mol ratio, we can distinguish brackish waters dissolving evaporites ( $\delta^{37}\text{Cl}$  near  $-1\text{\textperthousand}$  and high chlorine concentrations; Stewart and Spivack 2004) from other samples (Fig. 10a), confirming the inferences resulting from Br-I-Cl plots (Fig. 4). Samples are more scattered in the Br-Cl isotope plot (Fig. 10b), probably due to contribution of marine organogenic bromine (e.g. SALV), but most of them describe a rough positive trend with  $\sim 0.5$  slope. This is probably due to halogens diffusion from brines toward aquifers with lower salinities; in fact, the isotope fraction factor for chlorine diffusion is twice in comparison with bromine (Eggenkamp and Coleman 2009). This agrees with the lowest values of  $\delta^{37}\text{Cl}$  ( $-1.0$  to  $-1.4\text{\textperthousand}$ ) found in the spa's waters of the Romagna Adriatic coast, which is explainable with the chlorine diffusion from seawater (560 mM of Cl) or brine (2820 mM of Cl) with  $\delta^{37}\text{Cl} \cong 0\text{\textperthousand}$  into a brackish water with a Cl content from 28 to 282 mM and with a diffusion coefficient of about  $D_{37}/D_{35} = 0.9988$  (Appelo 2002).

## 5.7 Isotope Composition of Dissolved Strontium

The Miocene origin of the dissolved strontium in the brine waters of the Po plain inferred by Toscani et al. (2007) is substantially confirmed (Fig. 11), with some additional features. Salsomaggiore and Fontevivo brines could derive from: (1) a pre-Messinian/Middle Miocene evaporated seawater like interstitial waters in Western Mediterranean Basin (Vengosh et al. 1994); (2) Messinian seawater like MONT brine. The latter hypothesis would indicate that brines modified their strontium isotope composition after seawater evaporation due to intense water–rock interaction with the turbidites of the foredeep basin (Langhian-Serravallian) where they still reside after the intense intra-Messinian tectonic pulse and subsequent subsidence (Artoni et al. 2004, 2007). A similar shift toward lower strontium isotope value is shown also by brine waters of Messinian origin in Israel (Starinsky et al. 1983).

Waters from the Tuscan side of Apennine and Bobbio tectonic window show a more radiogenic  $^{87}\text{Sr}/^{86}\text{Sr}$  due to the interaction with flyschoid and/or metamorphic rocks of the area (Verrucano Formation for BERG spring; Paleozoic basement and/or arenaceous formations for BOB and SALMIN samples).

## 6 Conclusions

Chemical and isotope data from this study evidence some noteworthy features of the salt waters of the Northern Apennine and Po Plain: (1) Brines from the Northern Apennine Foredeep Basin are derived from Miocene seawater evaporated up to a stage between gypsum and halite saturation and then are diluted by Miocene or present-day waters of meteoric origin; the percentage of mixed meteoric water is higher in saline and brackish samples. Quite minor or no trace of fossil seawater was revealed in the brackish waters from Tuscan side (BERG, PM) or interacting with rocks of the Tuscan Nappe in the Emilia side of the Northern Apennine (SALMIN, BOB, F15), therefore their salinization derive exclusively by salt dissolution. (2) Decomposition of organic matter during burial and diagenesis is responsible for the high I and Br content, hydrocarbon formation and consumption of dissolved sulfate. Other diagenetic reactions such as dolomitization/chloritization (Mg-decrease, Ca-increase; Salsomaggiore, Cortemaggiore), albitization/

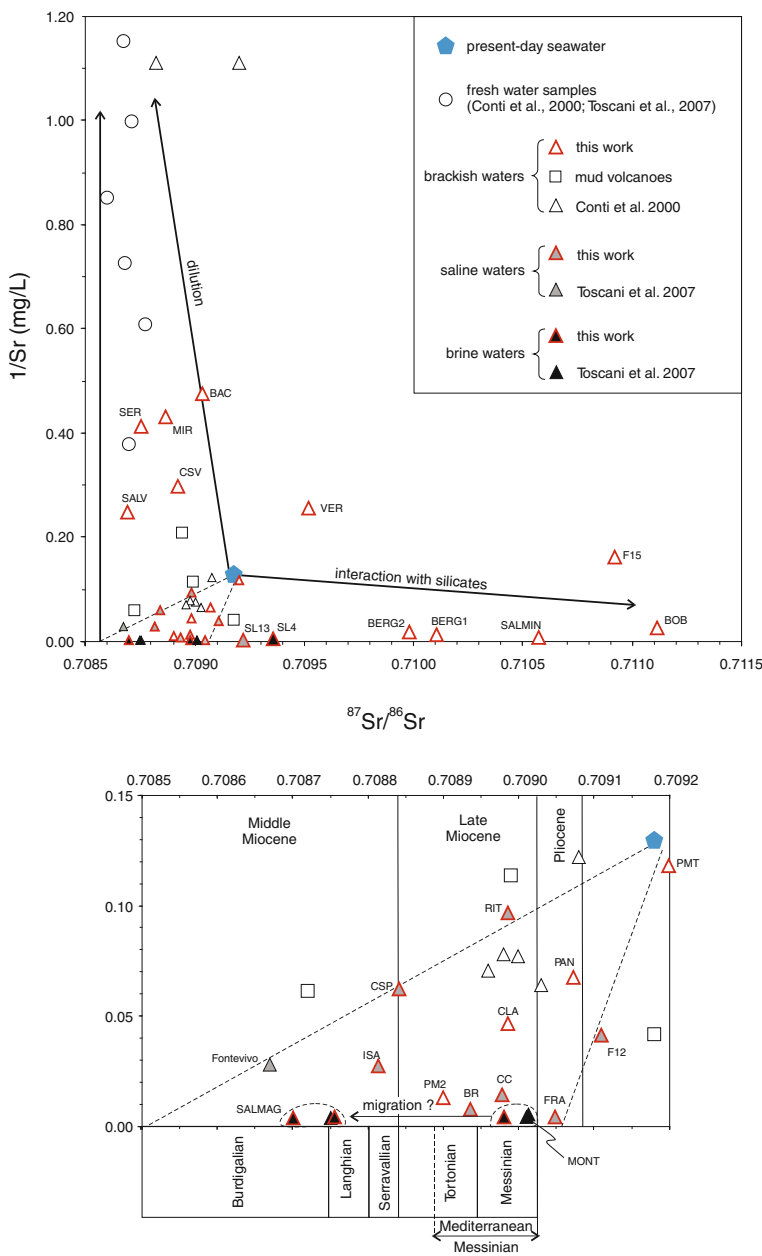


**Fig. 11**  $^{87}\text{Sr}/^{86}\text{Sr}$  versus  $1/\text{Sr}$  diagram for the salt waters from Northern Apennines and Po Basin. Global seawater strontium ratio timescale using nanofossils (McArthur et al. 2001) and range of values for Mediterranean during Messinian using evaporites (Matano et al. 2005) are also reported

zeolitization (Na-decrease, Ca-increase; Tolentino) and illitization/K-feldspar precipitation (K decrease) have modified the early composition of the waters. The ternary mixing between seawater, meteoric water and a diagenetic-related component derived from clay

and gypsum dehydration may explain the isotope composition of the mud volcanoes and brackish waters of similar origin (SALV). (3) Interestingly, gas-souring reaction could generate water with an oxygen isotope composition similar to the diagenetic end-member. Other data and studies are necessary to evaluate the amplitude of this process. (4) Among investigated brines from the Northern Apennine Foredeep, only Salsomaggiore shows an extreme  $\delta^{18}\text{O}$ -shift from meteoric water line: the high temperature of dolomitization or carbonate cement recrystallization suffered by the aquifer can explain the anomalous isotopic feature. Actually, the structural history of the Salsomaggiore basin is peculiar because it underwent a deep burial as a consequence of the progressive piling of the Ligurian/epi-Ligurian allochthonous units occurring in the late Messinian (Artoni et al. 2004). Considering the thickness of the eroded Ligurian/epi-Ligurian cover (2.5 km) and the maximum depth of the borehole intercepting brine (2.5 km; Campore Well), we obtain 5.0 km as palaeo-depth of the buried structure of Salsomaggiore, according to the geothermometric estimation of this study ( $\approx 150^\circ\text{C}$ ) and the maximum/present-day geothermal gradient ( $30^\circ\text{C}/\text{km}$ ). Moreover, a maximum depth of 7.5 km is obtained using the minimum/ancient ( $20^\circ\text{C}/\text{km}$ ) geothermal gradient of the area valid for fresh sediments during the basin filling (Cataldi et al. 1995; Wygrala 1987; Pieri 2001).

As future prospect, water dating by short-lived radiogenic isotope ( $^3\text{H}$  and  $^{14}\text{C}$ ) could clarify the potential input of present meteoric water, whereas long-lived radiogenic isotope ( $^{129}\text{I}$  and  $^{36}\text{Cl}$ ) could confirm or rule out the possible relation of the saline waters-brines from Northern Apennine Foredeep with a pre-Messinian evaporitic event like that invoked for the genesis of interstitial waters found in the Provence Basin (W-Mediterranean).

**Acknowledgments** The work was partly funded by the MURST-PRIN2005 project. Many thanks to all University of Parma fellows involved in the analytical works: Monica Maffini and Marinella Chierici for support on chemical, Silvia Vaccari for radon, Enrico Selmo for water isotope analyses. Special thanks to Liliana Krotz and Guido Giazzì, Thermo Scientific—Rodano, Milano, for total C and total N analyses. Reviews by two anonymous referees were greatly appreciated.

## References

- AGIP Mineraria (1959) I giacimenti gassiferi dell'Europa Occidentale. Accademia Nazionale dei Lincei and ENI, Roma
- Apha-Awwa-Wef (1995) Standard methods for the examination of water and wastewater, 19th edn. American Public Health Association, American Water Works Association, Water Environment Federation, USA
- Appelo CAJ (2002) Calculating the fractionation of isotopes in hydrochemical (transport) processes with PHREEQC-2. In: Schulz HD, Hadeler A (eds) Geochemical processes in soil and groundwater. GeoProc, Wiley-VCH, Weinheim, pp 383–398
- Argnani A, Ricci Lucchi F (2001) Tertiary siliciclastic turbidite systems of the Northern Apennine. In: Vai GB, Martini IP (eds) Anatomy of an orogen: the apennines and adjacent mediterranean basins. Kluwer, Dordrecht, pp 327–349
- Artoni A, Papani G, Rizzini F, Calderoni M, Bernini M, Argnani A, Roveri M, Rossi M, Rogledi S, Gennari R (2004) The Salsomaggiore structure (Northwestern Apennine foothills, Italy): a Messinian mountain front shaped by mass-wasting products. *Geo Acta* 3:107–127
- Artoni A, Rizzini F, Roveri M, Gennari R, Manzi V, Papani G, Bernini M (2007) Tectonic and Climatic Controls on Sedimentation in Late Miocene Cortemaggiore Wedge-Top Basin (Northwestern Apennines, Italy). In: Lacombe O, Lavé J, Roure F, Vergès J (eds) Thrust belts and foreland basins—from fold kinematics to hydrocarbon systems. Frontiers In Earth Sciences. Springer, Berlin, pp 431–456
- Artusi GC, De Marchi A, Marenghi I, Tagliavini S, Zanzucchi G (1977) The mineral waters of the Parma province. Origin composition and classification. Università degli Studi di Parma, Italy

- Bein A, Dutton AR (1993) Origin, distribution, and movement of brine in the Permian Basin (U.S.A.): a model for displacement of connate brine. *Geol Soc Am Bull* 105:695–707
- Bellanca A, Neri R (1986) Evaporite carbonate cycles of the Messinian, Sicily: stable isotopes, mineralogy, textural features, and environmental implications. *J Sediment Petrol* 56:614–621
- Bellia S, Censi P (1985) Il Messiniano evaporitico della Sicilia Orientale: l'ambiente di formazione dei gessi di Calatabiano (CT) sulla base di evidenza tessiturali e geochimica-isotopiche. *Miner Petrogr Acta* 29:61–74
- Bencini A, Duchi V, Martini M (1977) Geochemistry of thermal springs of Tuscany (Italy). *Chem Geol* 19:229–252
- Bonini M (2007) Interrelations of mud volcanism, fluid venting, and thrust-anticline folding: Examples from the external northern Apennines (Emilia-Romagna, Italy). *J Geophys Res* 112:B08413. doi: [10.1029/2006JB004859](https://doi.org/10.1029/2006JB004859)
- Borgia GC, Elmi C, Ricchiuto T (1988) Correlation by genetic properties of the shallow gas seepages in the Emilian Apennines (Northern Italy), in Advances in Organic Geochemistry 1987. *Org Geochem* 13:319–324
- Boschetti T (2003) Studio geochimico e geochimico-isotopico di acque a composizione estrema e termali dell'Appennino Settentrionale. Dissertation, University of Parma, Italy
- Boschetti T, Venturelli G, Toscani L, Barbieri M, Mucchino C (2005) The Bagni di Lucca thermal waters (Tuscany, Italy): an example of Ca-SO<sub>4</sub> waters with high Na/Cl and low Ca/SO<sub>4</sub> ratios. *J Hydrol* 307(1–4):270–293
- Boschetti T, Cortecchi C, Toscani L, Iacumin P (2010) Sulfur and oxygen isotope compositions of Upper Triassic sulfates from Northern Apennines (Italy): palaeogeographic and hydrogeochemical implications. *Geologica Acta* (in press)
- Böttcher ME, Brumsack HJ, De Lange GJ (1998) Sulfate reduction and related stable isotope (<sup>34</sup>S, <sup>18</sup>O) variations in interstitial waters of the eastern Mediterranean. In: Robertson AHF, Emeis KC, Richter C, Camerlenghi A (eds) Proceedings of the ocean drilling program, scientific results 160, College Station, TX, pp 365–373
- Böttcher ME, Bernasconi S, Brumsack HJ (1999) Carbon, sulfur and oxygen isotope geochemistry in interstitial waters from the western Mediterranean. In: Zahn R, Comas MC, Klaus A (eds) Proceedings of the Ocean Drilling Program, Scientific Results 161, College Station, TX, pp 413–422
- Brunner B, Bernasconi S, Kleikemper J, Schroth MH (2005) A model for oxygen and sulphur isotope fractionation in sulfate during bacterial sulfate reduction processes. *Geochim Cosmochim Acta* 20:4733–4785
- Capozzi R, Picotti V (2002) Fluid migration and origin of a mud volcano in the Northern Apennines (Italy): the role of deeply rooted normal faults. *Terra Nova* 14:363–370
- Carpenter AB (1978) Origin and chemical evolution of brines in sedimentary basins. *Oklah Geol Surv Circ* 79:60–77
- Cataldi R, Mongelli F, Squarci P, Taffi L, Zito G, Calore C (1995) Geothermal ranking of Italian territory. *Geothermics* 24:115–129
- Censi P (1984) Isotopic composition of water of crystallization of Sicilian selenitic gypsum crystals: interpretation of observed variations. *Miner Petrogr Acta* 28:139–153
- Censi P (1986) Frazionamento isotopico dell'ossigeno nell'acqua di cristallizzazione dei gessi e kainite di origine evaporitica. *Rend Soc It Min Petr* 41:273–279
- Clark I, Fritz P (1997) Environmental Isotopes in hydrogeology. Lewis Publications, Boca Raton
- Conti S, Artori A, Piola G (2007) Seep-carbonates in a thrust-related anticline at the leading edge of an orogenic wedge: The case of the middle–late Miocene Salsomaggiore Ridge (Northern Apennines, Italy). *Sediment Geol* 199:233–251
- Coplen TB, Hanshaw BB (1973) Ultrafiltration by a compacted clay membrane—I. Oxygen and hydrogen isotopic fractionation. *Geochim Cosmochim Acta* 37:2295–2310
- Cortecchi G, Orlandi P (1975) Analisi isotopica di minerali solfatici associati a zolfo, sulfuri e calcare. *Rend Soc It Min Petr* 31:379–398
- Cortecchi G, Dinelli E, Boschetti T, Arbizzani P, Pompilio L, Mussi M (2008) The Serchio River catchment, northern Tuscany: geochemistry of stream waters and sediments, and isotopic composition of dissolved sulfate. *Appl Geochem* 23:1513–1543
- Dähllmann A, de Lange GJ (2003) Fluid-sediment interactions at Eastern Mediterranean mud volcanoes: a stable isotope study from ODP Leg 160. *Earth Planet Sc Lett* 212:377–391
- Davisson ML, Criss RE (1996) Na-Ca-Cl relations in basinal fluids. *Geochim Cosmochim Acta* 60:2743–2752
- Dolenec T, Pezdic J, Herle U (1996) Stable isotope study of the Adriatic Sea. *Acta Geol Hung* 39 (Isotope Workshop III Suppl):35–38

- Drever JI (1997) The geochemistry of natural waters: surface and groundwater environments, 3rd edn. Prentice Hall, Upper Saddle River
- Duchi V, Venturelli G, Boccasavia I, Bonicolini F, Ferrari C, Poli D (2005) Studio geochimico dei fluidi dell'Appennino Tosco-Emiliano-Romagnolo. *Boll Soc Geol It* 124:475–491
- Eggenkamp HGM (1994) The geochemistry of chlorine isotopes. Ph.D. Thesis. University of Utrecht, The Netherlands
- Eggenkamp HGM, Coleman ML (2009) The effect of aqueous diffusion on the fractionation of chlorine and bromine stable isotopes. *Geochim Cosmochim Acta* 73:3539–3548
- El Mugammar H, Shouakar-Stash O (2008) Strontium isotope analysis. Technical Procedure, Environmental Isotope Laboratory, Department of Earth and Environmental Sciences, University of Waterloo, Waterloo
- Emilia-Romagna R, ENI – AGIP (1998) Riserve idriche sotterranee della Regione Emilia-Romagna. In: Di Dio G (ed.) S.E.L.CA, Firenze, pp 120
- Epstein S, Mayeda T (1953) Variations of  $^{18}\text{O}/^{16}\text{O}$  ratio in natural waters. *Geochim Cosmochim Acta* 4:213–224
- Fontes JC, Matray JM (1993) Geochemistry and origin of formation brines from the Paris Basin, France. I. Brines associated with Triassic salts. *Chem Geol* 109:149–175
- Fritz P, Basharmal GM, Drimmie RJ, Ibsen J, Qureshi RM (1989) Oxygen isotope exchange between sulphate and water during bacterial reduction of sulphate. *Chem Geol (Isot Geosc Sec)* 79:99–105
- Galley MR, Miller AI, Atherley JF, Mohn M (1972) GS process-physical properties. Chalk River, Ontario, Canada, Atomic Energy of Canada Limited, AECL-4225
- Gat JR, Carmi I (1970) Evolution in the isotopic composition of atmospheric waters in the Mediterranean Sea area. *J Geophys Res* 75:3039–3048
- Gavrieli I, Starinsky A, Spiro B, Ainzenshtat Z, Nielsen H (1995) Mechanisms of sulfate removal from subsurface calcium chloride brines; Heletz-Kokhav oilfields, Israel. *Geochim Cosmochim Acta* 59:3525–3533
- Gran G (1952) Determination of the equivalence point in the potentiometric titrations. *Analyst* 77:661–671
- Hanor JS (1987) Origin and migration of subsurface sedimentary brines. SEPM Short Course No. 21, U.S.A
- Horita J (2009) Isotopic evolution of saline lakes in the low-latitude and polar regions. *Aquat Geochem* 15:43–69
- Horita J, Wesolowski DJ (1994) Liquid-vapor fractionation of oxygen and hydrogen isotopes of water from the freezing to the critical temperature. *Geochim Cosmochim Acta* 58:3425–3437
- Horita J, Cole DR, Wesolowski DJ (1993) The activity-composition relationship of oxygen and hydrogen isotopes in aqueous salt solutions: II. Vapor-liquid water equilibration of mixed salt solutions from 50 to 100°C and geochemical implications. *Geochim Cosmochim Acta* 57:4703–4711
- Hutcheon I (2002) Principles of diagenesis and what drives mineral change. In: Kyser K (ed) Fluids and basin evolution, short course series, vol 28. Mineralogical Association of Canada, Ottawa, pp 93–114
- Hyeong K, Capuano RM (2001) Ca/Mg of brines in Miocene/Oligocene clastic sediments of the Texas Gulf Coast: buffering by calcite/disordered dolomite equilibria. *Geochim Cosmochim Acta* 65:3065–3080
- Hyeong K, Capuano RM (2004) Hydrogen isotope fractionation factor for mixed-layer illite/smectite at 60° to 150°C: new data from the northeast Texas Gulf Coast. *Geochim Cosmochim Acta* 68:1529–1543
- Iacumin P, Venturelli G, Burroni B, Toscani L, Selmo E (2007) The S. Andrea Bagni waters (Province of Parma): origin, mixing with high-salinity waters and inferences on climatic microvariations. *Mem Descrittive Carta Geol Italia* 76:219–228
- Iacumin P, Venturelli G, Selmo E (2009) Isotopic features of rivers and groundwater of the Parma Province (Northern Italy) and their relationships with precipitation. *J Geochem Expl* 102:56–62
- Kharaka YK, Mariner RH (1989) Chemical geothermometers and their application to formation waters from sedimentary basins. In: Naeser ND, McCollum TH (eds) Thermal history of sedimentary basins. Springer-Verlag, New York, pp 99–117
- Land LS, Macpherson GL (1992) Geothermometry from brine analyses: lessons from the Gulf Coast, U.S.A. *Appl Geochem* 7:333–340
- Lloyd RM (1967) Oxygen-18 composition of oceanic sulfate. *Science* 156:1228–1231
- Long G, Neglia S (1968) Composition de l'eau interstitielle des argiles et diagenèse des minéraux argileux. *Revue de l'Institut Français du Pétrole* 23:53–70
- Longinelli A (1979) Isotope geochemistry of some messinian evaporites: paleoenvironmental implications. *Palaeogeogr Palaeocl* 29:95–123
- Longinelli A, Flora O (2007) Isotopic composition of gypsum samples of Permian and Triassic age from the northeastern Italian Alps: palaeoenvironmental implications. *Chem Geol* 245:275–284

- Longinelli A, Ricchiuto TE (1977) Il ruolo delle acque meteoriche durante la crisi di salinità del Messiniano. *Boll Soc Geol It* 96:423–428
- Longinelli A, Selmo E (2003) Isotopic composition of precipitation in Italy: a first overall map. *J Hydrol* 270:75–88
- Longstaffe FJ (2000) An introduction to stable oxygen and hydrogen isotopes and their use as fluid tracers in sedimentary systems. In: Kyser K (ed) Fluids and basin evolution, short course series, vol 28. Mineralogical Association of Canada, Ottawa, pp 115–162
- Lu FH, Meyers WJ (2003) Sr, S, and  $\text{O}_{\text{SO}_4}$  Isotopes and the Depositional Environments of the Upper Miocene Evaporites, Spain. *J Sediment Res* 73:444–450
- Lu FH, Meyers WJ, Schoonen MA (2001) S and O isotopes and their quantitative modeling of late Miocene gypsum, Nijar, Spain. *Geochim Cosmochim Acta* 65:3081–3092
- Machel HG (2001) Bacterial and thermochemical sulfate reduction in diagenetic settings—old and new insights. *Sediment Geol* 140:143–175
- Maekawa T, Imai N (2000) Hydrogen and oxygen isotope fractionation in water during gas hydrate formation. In: Holder GD, Bishnoi PR (eds) Gas hydrates: challenges for the future, Annals of the New York Academy of Sciences. New York Academy of Sciences, New York, pp 452–459
- Martin JB, Gieskes JM, Torres M, Kastner M (1993) Bromine and iodine in Peru margin sediments and pore fluids—implications for fluids origins. *Geochim Cosmochim Acta* 57:4377–4389
- Martinelli G, Dadomo A (2005) Geochemical model of mud volcanoes from reviewed worldwide data. In: Martinelli G, Panahi B (eds) Mud volcanoes, geodynamics and seismicity. Springer, the Netherlands, pp 211–220
- Matano F, Barbieri M, Di Nocera S, Torre M (2005) Stratigraphy and strontium geochemistry of Messinian evaporite-bearing successions of the southern Apennines foredeep, Italy: implications for the Mediterranean “salinity crisis” and regional palaeogeography. *Palaeogeogr, Palaeocat, Palaeoec* 217:87–114
- Mattavelli L, Margarucci V (1992) Malossa Field—Italy, Po Basin. In: Foster NH, Beaumont EA (eds) Treatise of petroleum geology, atlas of oil and gas field, structural traps VII. American Association of Petroleum Geologists, Tulsa, pp 119–133
- Mattavelli L, Ricchiuto T, Grignani D, Schoell M (1983) Geochemistry and habitat of natural gases in Po Basin, Northern Italy. *AAPG Bull* 67:2239–2254
- McArthur JM, Howart RJ, Bayley TR (2001) Strontium isotope stratigraphy: LOWESS version 3: best fit to the marine Sr-isotope curve for 0–509 Ma and accompanying look-up table for deriving numerical age. *J Geol* 109:155–170
- Milliken KL, McBride EF, Cavazza W, Cibin U, Fontana D, Picard MD, Zuffa GG (1998) Geochemical history of calcite precipitation in Tertiary sandstones, Northern Apennines, Italy. In: Morad S (ed) Carbonate Cementation in Sandstones, IAS Special vol 26, pp 213–240
- Molli G (2008) Northern Apennine-Corsica orogenic system: an updated overview. In: Diegesmund S, Füdenschuh B, Froitzheim N (eds) “Tectonic aspects of the Alpine-Dinaride-Carpathian System”. *Geol. Soc. London Spec. Pub.* 298, pp 413–442
- Morad S, Worden RH, Ketzer JM (2003) Oxygen and hydrogen isotope composition of diagenetic clay minerals in sandstones: a review of the data and controls. In: Worden RH and Morad S (eds) Clay Mineral Cement in Sandstones, IAS Special vol 34, pp 63–92
- Nadler A, Magaritz M (1980) Studies of marine solution basins—isotopic and compositional changes during evaporation. In: Nissenbaum A (ed) Hypersaline brines and evaporitic environments, developments in sedimentology. Elsevier, Amsterdam, pp 115–129
- Nanni T, Vivalda P (1999) Le acque saline dell’avanfossa marchigiana: origine, chimismo e caratteri strutturali delle zone di emergenza. *Boll Soc Geol It* 118:191–215
- O’Neil JR, Clayton RN, Mayeda TK (1969) Oxygen isotope fractionation in divalent metal carbonates. *J Chem Phys* 51:5547–5558
- Olivero GF, Zauli M, Zuppi GM, Ricchiuto TE (1987) Isotopic composition and origin of sulphur compounds in groundwaters and brines in the Po Valley (Northern Italy). In: Studies On Sulphur Isotope Variations in Nature. IAEA, Vienna, pp 49–64
- Parkhurst DL, Appelo CAJ (1999) User’s guide to PHREEQC (version 2)—A computer program for speciation, batch reaction, one-dimensional transport and inverse geochemical calculations. Water Resources Investigations Report, 95-4259. US Geological Survey
- Picotti V, Capozzi R, Bertozzi G, Mosca F, Sitta A, Tornaghi M (2007) The Miocene Petroleum System of the Northern Apennines in the Central Po Plain (Italy). In: Lacombe O, Lavé J, Roure F, Vergés J (eds) Thrust belts and foreland basins—from fold kinematics to hydrocarbon systems. Frontiers in earth sciences. Springer, Berlin, pp 117–131

- Pieri M (1992) Cortemaggiore Field—Italy, Po plain, Northern Apennines. In: Foster NH, Beaumont EA (eds) Treatise of petroleum geology, atlas of oil and gas field, structural traps VII. AAPG, Tulsa, pp 99–118
- Pieri M (2001) Italian Petroleum Geology. I. In: Vai GB, Martini IP (eds) Anatomy of an orogen: the apennines and adjacent mediterranean basins. Kluwer, Dordrecht, pp 533–549
- Pierre C (1982) Teneurs en isotopes stables ( $^{18}\text{O}$ ,  $^2\text{H}$ ,  $^{13}\text{C}$ ,  $^{34}\text{S}$ ) et conditions de genèse des évaporites marines: application à quelques milieux actuels et au Messinien de Méditerranée [Doct. thesis]. Univ. Paris-Sud Orsay
- Pierre C, Catalano R (1976) Stable isotopes ( $^{18}\text{O}$ ,  $^{13}\text{C}$ ,  $^2\text{H}$ ) in the evaporitic sequence of the Ciminna basin (Sicily). In: Catalano R, Ruggieri G, Sprovieri R (eds) Messinian evaporites in the Mediterranean. Memorie Società Geologica Italiana 16:55–62
- Pierre C, Rouchy JM (1990) Sedimentary and diagenetic evolution of Messinian evaporites in the Tyrrhenian Sea (ODP Leg 107, Sites 652, 653, and 654): petrographic, mineralogical, and stable isotope records. In: Kastens KA, Mascle J, et al (eds) Proceedings of the ocean drilling program, scientific results, 107, pp 187–210
- Ricchiuto T, McKenzie JA (1978) Stable isotope investigation of Messinian sulfate samples from DSDP Leg 42 A, eastern Mediterranean Sea. In: Hsu KJ, Montadert L et al (eds) Initial Report of the DSDP 42 (Part 1). U.S. Govt. Printing Office, Washington, pp 657–660. doi:[10.2973/dsdp.proc.42-1.126-2.1978](https://doi.org/10.2973/dsdp.proc.42-1.126-2.1978)
- Ricchiuto T, Zuppi GM, Bortolami GC, Olivero GF (1985) Le acque salate della Pianura Padana. Parte I Inquadramento Geochimico. In: Francani V, Zuppi GM (eds) Studi idrogeologici sulla Pianura Padana 1, Clup, Milano, pp 9–30
- Ricci Lucchi F (1981) The Marnoso-arenacea turbidites, Romagna and Umbria Apennines. In: Ricci Lucchi F (ed) Excursion guidebook, with contribution on sedimentology of some Italian basins. 2nd IAS Eur. Meeting, Bologna, pp 229–303
- Rosenthal E (1997) Thermomineral water of Ca-chloride composition: review of diagnostics and of brine evolution. Environ Geol 32:245–250
- Rosetti E, Valenti L (2002) Terme e acque segrete dell'Emilia Romagna. Le Lettere, Firenze
- Roveri M, Bassetti MA, Ricci Lucchi F (2001) The Mediterranean Messinian salinity crisis: an Apennine foredeep perspective. Sed Geol 140:201–214
- Roveri M, Manzi V, Lucchi FR, Rogledi S (2003) Sedimentary and tectonic evolution of the Vena del Gesso basin (Northern Apennines, Italy): implications for the onset of the Messinian salinity crisis. Geol Soc Am Bull 115:387–405
- Rozanski K, Araguas-Araguas L, Gonfiantini R (1993) Isotopic patterns in modern global precipitation. In: Swart PK, Lohman KL, McKenzie JA, Savin S (eds) Climate change in continental isotopic record. Geoph Monograph vol. 78, pp 1–37
- Sborgi U, Galanti A, Conti Z (1936) Analisi chimica e chimico-fisica dell'acqua minerale di Fontevivo (Parma). Ann Chim Appl 26:502–515
- Schoeller H (1962) Les eaux souterraines. Masson, Paris
- Seal RR II, Alpers CN, Rye RO (2000) Stable isotope systematics of sulfate minerals. In: Alpers CN, Jambor JL, Nordstrom DK (eds) Sulfate Minerals: Crystallography, Geochemistry, and Environmental Significance. Reviews in Mineralogy and Geochemistry, vol 40, Mineralogical Society of America and Geochemical Society, Washington, D.C., pp 541–602
- Sharp Z (2007) Principles of stable isotope geochemistry. Pearson Prentice Hall, Upper Saddle River
- Shouakar-Stash O, Frape SK, Drimmie RJ (2005a) Determination of bromine stable isotopes using continuous-flow isotope ratio mass spectrometry. Anal Chem 77:4027–4033
- Shouakar-Stash O, Drimmie RJ, Frape SK (2005b) Determination of inorganic chlorine stable isotopes by Continuous Flow Isotope Ratio Mass spectrometry. Rapid Commun Mass Spectrom 19:121–127
- Siemann MG, Schramm M (2000) Thermodynamic modelling of the Br partition between aqueous solutions and halite. Geochim Cosmochim Acta 64:1681–1693
- Starinsky A, Bielsky M, Lazar B, Steinitz G, Raab M (1983) Strontium isotope evidence on the history of oilfield brines, Mediterranean Coastal Plain, Israel. Geochim Cosmochim Acta 47:687–695
- Stewart MA, Spivack AJ (2004) The Stable-Chlorine isotope composition of natural and anthropogenic materials. In: Johnson CM, Beard BL, Albareda F (eds) Geochemistry of non-traditional stables isotopes, Reviews in Mineralogy & Geochemistry 55. Mineralogical Society of America and the Geochemical Society, Washington D.C., pp 231–254
- Thode HG, Monster J (1965) Sulfur isotope geochemistry of petroleum, evaporites and ancient seas. In: Young A, Galley JE (eds) Fluids in Subsurface Environments, AAPG Memoir 4, Tulsa, Oklahoma, pp 367–377
- Toscani L, Venturelli G, Boschetti T (2001) Sulphide-bearing waters in Northern Apennines, Italy: general features and water rock interaction. Aquat Geochem 7:195–216

- Toscani L, Boschetti T, Maffini M, Barbieri M, Mucchino C (2007) The groundwaters of Fontevivo (Parma Province, Italy): redox processes and mixing with brine waters. *Geochem-Explor Env A* 7:23–40
- Vaccari S, Toscani L, Ortalli I, Dalle Donne C, Martinelli G, Venturelli G (1999) Misure di radon in sorgenti e pozzi dell'Appennino Reggiano-Parmense. *Quad Geol Appl* 2:3315–3320 (1999 supplementary volume)
- Van der Weijden C (1992) Early diagenesis and marine pore water. In: Wolf KH, Chilingarian GV (eds) Diagenesis III. Elsevier, Amsterdam, pp 1–134
- Vengosh A, Starinsky A, Anati DA (1994) The origin of Mediterranean interstitial waters—relics of ancient Miocene brines: a re-evaluation. *Earth Planet Sc Lett* 121:613–627
- Vengosh A, Gieskes J, Mahn C (2000) New evidence for the origin of hypersaline pore fluids in the Mediterranean basin. *Chem Geol* 163:287–298
- Venturelli G (2003) Acque, minerali e ambiente. Fondamenti di geochimica dei processi di bassa temperatura. Pitagora, Bologna
- Venturelli G, Boschetti T, Duchi V (2003) Na-carbonate waters of extreme composition: Possible origin and evolution. *Geochim J* 37:351–366
- Wolery TW, Jarek RL (2003) EQ3/6, version 8.0—Software User's Manual. Civilian Radioactive Waste Management System, Management & Operating Contractor. Sandia National Laboratories, Albuquerque, New Mexico
- Worden RH, Smalley PC, Oxtoby NH (1996) The effects of thermochemical sulfate reduction upon formation water salinity and oxygen isotopes in carbonate gas reservoirs. *Geochim Cosmochim Acta* 60:3925–3931
- Wygrala BP (1987) Integrated computer-aided basin modeling applied to analysis of hydrocarbon generation history in a Northern Italian oil field. *Org Geochem* 13:187–197
- Xie X, Jiu JJ, Li S, Cheng J (2003) Salinity variation of formation water and diagenesis reaction in abnormal pressure environments. *Sci China Ser D* 46:269–284